УНИВЕРЗИТЕТ У БЕОГРАДУ
ЕЛЕКТРОТЕХНИЧКИ ФАКУЛТЕТ

Мастер рад

УТИЦАЈ ПРОСТОРНОФРЕКВЕНЦИЈСКОГ ФИЛТРИРАЊА НА ОБРАДУ КОРТИКАЛНИХ СИГНАЛА ТОКОМ ЗАМИШЉАЊА ПОКРЕТА

Ментор:
Проф. др Дејан Поповић

Студент:
Бојана Мирковић
Бр. индекса: 2012/3141

Београд, јул 2013.

UNIVERSITY OF BELGRADE
SCHOOL OF ELECTRICAL ENGINEERING

Master thesis

THE IMPACT OF SPATIO-SPECTRAL FILTERING FOR MOTOR IMAGERY

Mentor:
Prof. Dr Dejan Popović

Student:
Bojana Mirković
Student ID: 2012/3141

In Belgrade, July 2013

ACKNOWLEDGEMENTS

Before I start I will take some time to mention that this master thesis, other than being a product of my interest and curiosity, is also the result of successful collaboration between the School of Electrical Engineering, University of Belgrade and Department of Psychology, University of Oldenburg. Due to the hospitality of my German colleagues as well as their valuable suggestions and great attitude towards work as well as fun, this thesis has proven to be very interesting and scientifically satisfying.

I would like to thank Professor Maarten de Vos for all the support during all parts of this project and Professor Stefan Debener for inviting me to the Department of Psychology at University of Oldenburg, where all the EEG recordings for this master thesis have been done.

I would especially like to extend my gratitude to Professor Dejan Popović for his support during my bachelor and master studies, since his belief in my work and valuable comments have been of great help in the past few years, as well as for constantly reminding me of a long way still before me in this field.

Bojana Mirković

РЕЗИМЕ

Радозналост је једна од основних одлика сваког човека. Разумевање сложених појмова и идеја код човека ствара осећај задовољства и достигнућа који се не може поредити са много других осећаја. Мистерије тешке за разумевање, али не и немогуће, у својој сржи су најчешће о нама самима: како смо настали, шта представљамо, како наш ум функционише? Ово последње питање интригирало је научнике вековима, али дошло је време да смо у могућности да, до одређене тачке, схватимо природу човечјег мозга и искористимо његове функције на потпуно нови начин.

За највећи део овог напретка заслужан је проналазак електроенцефалографије (ЕЕГ), технике која бележи електричну активност мозга. Она нам је пружила увид у рад човечјег мозга. Иако још увек не можемо потпуно разумети свој ум услед његове сложености, ЕЕГ нам омогућава да сакупимо корисне информације које су временом биле довољне да нас доведу до проналаска првих система за интеракцију између човека и рачунара путем можданих сигнала (*енг. Brain-Computer Interface, BCI*). Ова технологија, која се ослања на ЕЕГ сигнале, данас може да се користи да омогући пацијентима у поодмаклој фази амиотрофичне латералне склерозе (АЛС) да комуницирају, пружи пацијентима који су доживели мождани удар средства којима би потенцијално повратили изгубљене функције, или чак може бити комерцијално коришћена у производњи рачунарских игара.

Једна од најзначајнијих парадигми које се користе у *BCI* системима је замишљање покрета, односно ментални процес у коме појединац симулира задату радњу. Ова радња може на пример бити покрет леве или десне руке, који за потребе контроле рачунара путем *BCI* система, мора бити детектован и класификован као такав из ЕЕГ сигнала. Прецизна класификација ових кортикалних сигнала у великој мери зависи од фреквенцијске и просторне филтрирације, али и од самог ЕЕГ мерења и парадигме која се у ту сврху користи. У овом раду акценат ће бити управо на методама којима се проценат тачне класификације може повећати, како софтверским, тако и хардверским.

Обзиром на то да је висок квалитет ЕЕГ записа веома важан предуслов прецизне класификације, у првом делу рада предложена је реалистична визуелна повратна информација током ЕЕГ сесије кориснику система. Ова информација је у облику робота који изршава корисников замишљени покрет. Постоје теоријске основе, дате у претходним радовима, помоћу којих се може закључити да овакав приступ резултује бољом класификацијом од до сада коришћених повратних информација, услед повећања концентрације самог корисника на његов задатак. Овом проблему приступљено је првобитно са софтверске тачке гледишта, програмирањем неопходних апликација за контролу мотора робота путем сигнала који се симултано снимају системом за ЕЕГ аквизицију. У ову сврху коришћени су програмски пакети OpenViBE и Matlab (*енг. Matrix laboratory*). Након тога, робот је хардверски конфигурисан тако да његови покрети одговарају замишљеној радњи корисника.

У другом делу рада биће речи о посебно популарној техници за обраду ЕЕГ сигнала за потребе *BCI* система - *CSP* методи (*енг. Common Spatial Pattern*) као и њој сродној методи која комбинује просторне филтре из *CSP* методе са фреквенцијским филтрирањем, *CSSSP* (*Common Sparse Spatio Spectral Filtering*). Процена успешности обе методе биће одрађена у програмском језику *MATLAB* а њени резултати ће бити визуелизовани и дискутовани. Обзиром на то да се у својој основи проблем метода за одређивање просторних и фреквенцијских филтара своди на оптимизационе алгоритме, у раду ће бити анализиран метод његовог решавања помоћу карактеристичних вектора, а биће и представљен цео математички прорачун. У циљу најбоље класификације биће упоређени резултати добијени

помоћу просторног филтра и помоћу просторно-фреквенцијског филтра и биће приказане њихове предности и недостаци. Оба алгоритма су међу најчешће коришћеним алгоритмима у пракси, тако да на основу анализе извршене у овом раду може да се процени у којој прилици би требало који од њих користити.

Прво поглавље рада ће бити уводно и у њему ће бити речи о нервном систему човека и електроенцефалографији, док ће у другом поглављу бити представљени системи за интеракцију између човека и рачунара путем можданих сигнала. У овом поглављу биће анализиране предности и недостаци неких парадигми за замишљање покрета.

У трећем поглављу биће описана реализација ЕЕГ сесије са визуелном повратном информацијом пацијенту у облику робота (*енг. feedback*), неопходнхо програмирање и хардверска решења потребна за овакву сесију.

У четвртом поглављу ће бити детаљно објашњене просторне методе обраде ЕЕГ сигнала, а посебна пажња ће бити посвећена *CSP* методи и њој блиској методи просторнофреквенцијске филтрације *CSSSP*. Овде ће бити описно приказана и реализација оба алгоритма у програмском језику Matlab.

Пето поглавље ће садржати упоредну анализу ова два алгоритма, као и одабир фреквенцијског филтра којим се добија најбоља класификација можданих сигнала. У оквиру петог поглавља биће сумирани резултати анализе оба алгоритма са свим њиховим специфичностима и проблемима које носе.

Шесто и седмо поглавље чиниће закључак и списак коришћене литературе.

ABSTRACT

It is in basic human nature to be curious. Understanding complex terms and notions brings forth the feeling of satisfaction and accomplishment which can be compared to very few human sentiments. The mysteries which are hard but not impossible to understand more often than not involve ourselves: how we came into existence, what we are, how our mind works? The last question has intrigued scientists for centuries, but the time came when we are able to, up to a certain level, understand our brain and use its functions in a completely new manner.

Much of this progress is due to electroencephalography (EEG), a technique which records the brain's electrical activity, which has given us the insight to how our brain works. While we still cannot understand our mind in its full complexity, the EEG has provided us with valuable information which, with time, was sufficient to lead us to the invention of the first brain-computer interface (BCI) systems. This technology, which relies on EEG recorded signal, can nowadays be used to enable patients in a late stage of amyotrophic lateral sclerosis (ALS) or locked-in syndrome to communicate, provide post stroke patients with means to recover their lost functions or even be used for entertainment purposes in gaming industry.

One of the most important paradigms used in BCI systems is motor imagery, a mental process during which an individual simulates a given action. This action can for instance be left and right hand movement, which, for the purposes of controlling some action by means of the BCI system, must be detected and classified from the EEG signal. Accurate classification of these cortical signals largely relies on spectral and spatial filtering, but also on EEG measurement itself and the paradigm used during the EEG session. In this thesis both hardware and software methods which improve classification statistics will be described.

Considering that the high quality EEG signal is a prerequisite for accurate classification, in the first part of the thesis we propose a realistic visual feedback in the form of a robot. In this case, the role of the robot is to execute the user's imagined task. Based on previous findings, this approach has more potential for providing excellent classification results then other tested visual feedbacks, due to an increase of user's focus on the task. We programmed the necessary software for controlling the robot's motors during the EEG session in OpenViBE and Matlab programming packages and the programming process and requirements are described in the paper. Afterwards, we rebuilt the robot so its movements would correspond to the imagined movement of the user.

In the second part of the paper, a particularly popular and powerful signal processing technique for EEG-based BCIs called Common Spatial Patterns (CSP) will be discussed and compared to its novel method which combines the spatial filters from CSP with frequency filtering, Common Sparse Spatio Spectral Pattern (CSSSP). We did the evaluation of these two methods in the MATLAB programming language, and the results of the analyses will be visualized and discussed. Since the underlying problem of this method for determination of spatial and spectral filters comes down to the optimization algorithms, we also revised the eigenvector method and other mathematical solutions. Both of these spatial filtering algorithms are among most often used ones in practice, so the given analysis may offer an insight to the purpose and circumstances under which each of them is used.

The first chapter will be introductory, so a human nervous system and electroencephalography will be discussed, while in the second chapter BCI systems will be presented. In this chapter paradigms related to motor imagery, as well as their advantages and disadvantages will be analyzed.

The third chapter will contain the description of the visual robotic feedback, as well as the necessary programming and hardware solutions for the experimental setup.

In fourth chapter the spatial EEG signal processing methods will be explained in detail, and particular attention will be dedicated to the CSP method and its counterpart CSSSP, focused on spatio-spectral filtering. Here, the implementation of both of these algorithms in a programming language MATLAB will be presented.

The fifth chapter contains a comparative analysis of methods used for obtaining optimal EEG signals as well as the selection of frequency filter best suited for the most accurate classification. This chapter will summarize the results of the analysis of both algorithms.

The sixth and seventh chapter will be a conclusion and a list of references, respectively.

Contents

Nomenclature

a, b...	scalars
$\boldsymbol{A}$, $\boldsymbol{a}$, $\boldsymbol{B}$, $\boldsymbol{b}$...	matrices/vectors/arrays
$\boldsymbol{A}_{ij}$, $\boldsymbol{a}_{ij}$ ...	element of a given matrix at position (i, j)
$\boldsymbol{A}^T$, $\boldsymbol{a}^T$...	transpose matrix
$\boldsymbol{A}$(n), $\boldsymbol{a}$(n)	n-th element of array
$\boldsymbol{I}$	identity matrix
$\mathbb{R}$	the set of real numbers
$trace(\boldsymbol{A})$	trace of the matrix
$dim(\boldsymbol{A})$	dimension of vector $\boldsymbol{A}$
:=	identity
$\sum$	sum
$\in$	element of
$\begin{bmatrix}\boldsymbol{A}\\ \boldsymbol{B}\end{bmatrix}$	vertical concatenation of two matrices

Abbreviations

ALS	Amyotrophic Lateral Sclerosis
ASD	Autism Spectrum Disorder
CMRR	Common-Mode Rejection Ratio
CSP	Common Spatial Patterns
CSP	Common Spatial Pattern
CSSP	Common Spatio-Spectral Pattern
CSSSP	Common Sparse Spatio Spectral Pattern
ERD	Event Related Desynchronization
ERP	Event Related Potential
ERS	Event Related Synchronization
ICA	Inependant Component Analysis

List of tables

List of figures

1. INTRODUCTION

In this chapter the physiology of the human brain will be presented and the general background of the human nervous system and brain as its most important part will be described. We will summarize the important physiological aspects in order to better explain the basics of electroencephalography (EEG). We will also discuss the EEG measurements, as well as the subsequent signal processing and the application of processed data. Finally, the aims of the thesis will be outlined at the end of the chapter.

1.1. Physiological background

Human brain consists of billions of nerve cells, called neurons (Fig 1.1). The role of the neurons in the human nervous system is transmitting the information from the place where the certain event was detected (e.g. sense of touch) to the brain, and vice versa, to transmit information from the brain to the places on the periphery (e.g., movement initiation). This information is electrical in nature, in the form of an action potential, which stands for a membrane depolarization under external influence.

Neurons transmit action potential using proteins transported through their membrane. Under external influences these proteins govern the exchange of potassium and sodium between the neurons and the extracellular space, thus changing the polarization of the membrane, creating a membrane voltage at the place of origin.

From the place of origin the action potential is transferred to the adjacent part of the membrane by positive ion diffusion along the axon volume. That part of the axon is then depolarized as previously excited one is returned to equilibrium. In this manner signal spreads along the axon of the excited neurons.

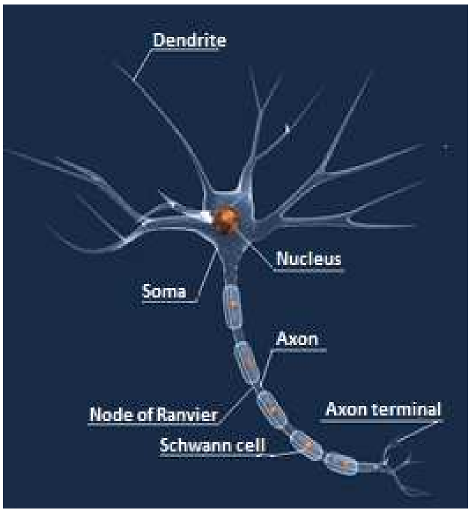

Figure 1.1. Neuron and its components

Transferring the signal from the axon of one cell to the dendrite of another occurs via synapses, the links between the neurons, due to the lack of continuity between the cytoplasm of nerve cells. When the electrical stimulation reaches the end of an axon of one neuron it triggers the chemical reaction releasing the neurotransmitters from the excited neuron into the synapse. The neurotransmitters then diffuse across the synapse. After entering the dendrite of postsynaptic neuron (which holds the receptors on the cell membrane) they generate an action potential in this cell [4]. Travelling through neurons and synapses, the action potential which originated at the periphery reaches the spine and from there it can either cause a reflex reaction, sending another action potential towards the periphery in response to the one that was received, or it can travel along the spinal cord and reach the body's main processing unit, the brain.

The number of neurons in the brain varies dramatically from species to species. One estimate puts the human brain at about 100 billion (10^{11}) neurons and 100 trillion (10^{14}) synapses [7]. The human brain has features which provide higher functions then most of the other animal brains. Among other things, this is due to the existence of an extremely developed cerebral cortex. In humans the cerebral cortex is so large that it overshadows every other part of the brain. It is a sheet of neural tissue, folded in a way that allows a large surface area to fit within the confines of the skull. When unfolded, each cerebral hemisphere has a total surface area of about 0.12 m^2 [8].

The cerebral cortex is nearly symmetrical. Left and right hemispheres are mirror images of each other, and each is responsible for the functions of the side of the body opposite to it. Each hemisphere is conventionally divided into four lobes: the frontal lobe, parietal lobe, occipital lobe, and temporal lobe (Fig 1.2). Division into lobes does not derive from the structure of the cortex itself, instead the lobes are named after the bones of the skull that overlie them, the frontal bone, parietal bone, temporal bone, and occipital bone. The borders between lobes lie beneath the sutures that link the skull bones together.

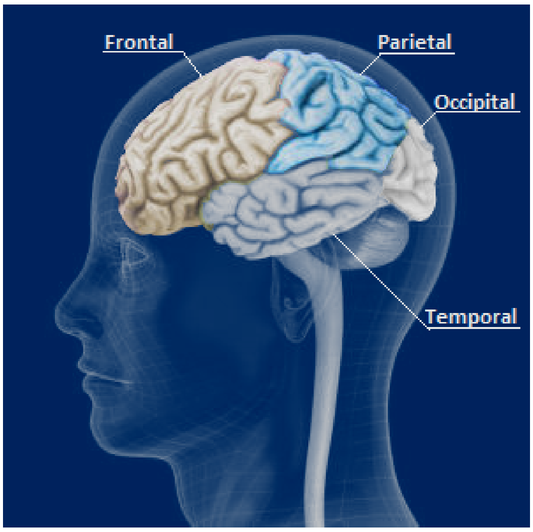

Figure 1.2. Brain lobes

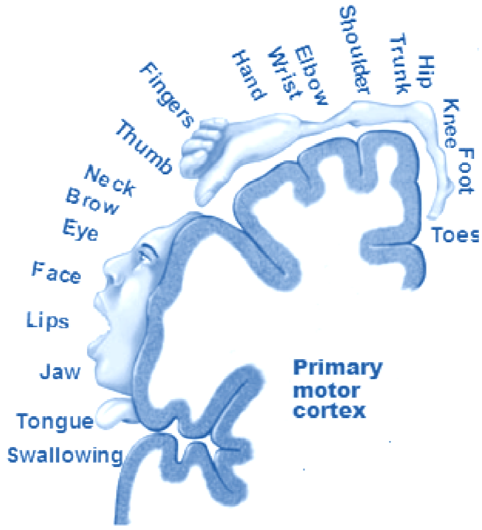

Figure 1.3 Motor homunculus

With the exception of the occipital lobe, a small area that is entirely dedicated to vision, each of the lobes contains a variety of brain areas that have minimal functional relationship. The parietal lobe contains areas involved in visuospatial tasks, including hand reaching, grasping, eye and attention orienting, mental rotation, and spatial working memory, but it's also in charge of mental calculation and phonological word processing [9]. The temporal lobe controls auditory and visual memories, language, and some hearing and speech [4]. The main functions of the frontal lobe are to control attention, abstract thinking, behavior, problem solving tasks, physical reactions and personality [10].

In the place where frontal and parietal lobes meet, along the fold in the cortex called the central sulcus, is the functional region called the sensorimotor cortex. The motor centers are all located here, controlling all the motor activities and movements, but can also be activated by movement imagination. Primary motor cortex, a strip of tissue running along the posterior portion of the frontal lobe, works in association with other motor areas and several subcortical brain regions, to plan and execute these movements.

Primary motor cortex contains a group of large neurons known as Betz cells. Betz cells, along with other cortical neurons, send long axons down the spinal cord to the synapse located there. From here the electrical stimulus travels through the interneuron circuitry in spine to the dendrites of alpha motor neurons in the spinal cord which connect to the muscles.

The primary motor cortex can be pictured as a rough map of the body, where different body parts specify which region of motor cortex they are controlled by. These regions are functionally partially overlapping in nature but roughly they are arranged from the toe which is controlled by top of the cerebral hemisphere, to mouth controlled by the bottom region of the hemisphere. Each cerebral hemisphere contains a map that controls mainly the opposite side of the body. This map is called the homunculus (Fig 1.3). This model is especially useful in estimation of activated brain areas during the EEG measurements.

1.2. Electroencephalography

As was already mentioned, neurons are constantly exchanging ions with the extracellular milieu, for example to maintain resting potential and to propagate action potentials. Therefore, neurons possess specific electrical property which allows them to produce electrical fields of various strengths depending on their activity. These fields may be recorded by means of electrodes at cortical surface or the patient's scalp. Electrodes are placed on the necessary places on the scalp and by measuring the difference in potentials in two places the EEG signal is formed.

1.2.1. EEG history

The first attempt at the electrical activity of the brain made a physician Richard Caton (1842-1926). Due to his profound interest in electrophysiological phenomena he received a grant from the British Medical Association to explore cerebral hemispheres of rabbits and monkeys. In his research Caton found that "feeble currents of varying direction pass through the multiplier when the electrodes are placed on two points of the external surface". This sentence is considered as the first step in electroencephalography. [3]

Since then and up until the World War I, there have been constant contributions to this branch from Eastern Europe. In 1890, Polish physiologist Adolf Beck published an investigation of spontaneous electrical activity of the brain of rabbits and dogs that included rhythmic oscillations altered by light. Two Russian physiologists made further studies along these lines: Pavel Yurevich Kaufman (1877-1951) and Vladimir Vladimirovich Pravdich-Neminsky (1879-1952). Neminsky began recording brain activity of the animals in 1912 with the galvanometer. His recordings were the first pictorial demonstration of EEG. Among other Russian neuroscientists who followed a similar path the most eminent was Vladimir Bechterev (1857-1927). However, when the Nobel Prize was awarded to Ivan Petrovich Pavlov for his early work on conditioned reflexes, all the work done by Bechterev was overshadowed and with it halted all neurophysiology progress in Russia.

When the electroencephalographic research went dormant in Eastern Europe, the Central Europe started flourishing. In 1924 German physiologist and psychiatrist Hans Berger (1873–1941) recorded the first human EEG. Berger's work was carried out in a small and very primitive laboratory. There, he conducted experiments involving the cerebral circulation. However, he also invented the electroencephalogram, giving the device its name, an invention described "as one of the most surprising, remarkable, and momentous developments in the history of clinical neurology".

Since the invention of electroencephalogram the neurosciences developed more rapidly. The differences in brain rhythms have been noted as well as the pathological states of the bran, but one of the most important events was the discovery of interictal spike as the focal signature of epilepsy.

The 1960s and 1970s witnessed a regrettable alienation of EEG and epileptology. The reasons for this could be various. Either way the situation changed in the 1980s due to the rapidly increasing emphases on EEG and related techniques in the presurgical workup of patients considered candidates for seizure surgery. [3]

Modern day electroencephalography does not differ much from the techniques used in the 1980s, however it is a tool which gives us the means of furthering our modest knowledge of the complex structure of human brain, improve the medical applications by discovering numerous new conditions and developing different scientific theories which bring us closer to complete understanding of our own bodies.

1.2.2. EEG equipment and instrumentation

In 1926, in Berger's time, the electrophysiological instrumentation consisted of a string galvanometer, which was later replaced by double coil galvanometer attaining a sensitivity of 130 µV/cm, and nonpolarizable pad electrodes. The records were made on photographic paper with recordings from 1 to 3 minute duration. At the time he was only able to record one channel using the bipolar recording technique with fronto-occipital leads [3]. This first recording was made in 1925 and is shown on top of Fig 1.4. Other than the EEG Berger recorded a sine wave for use as a time marker.

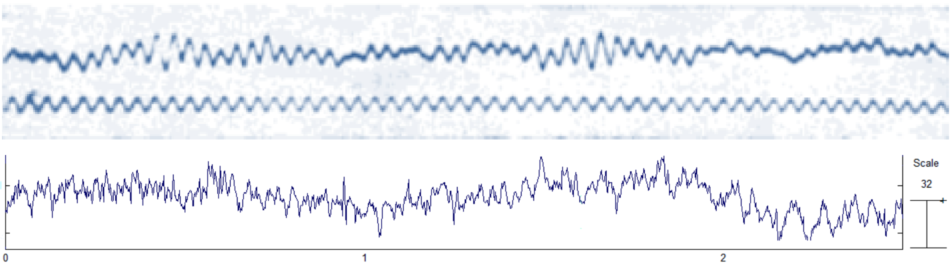

Figure 1.4. The first electroencephalogram of a human with the time marker below (top) in comparison to the raw EEG recording today (bottom)

Today, there is a clearly established set of rules and procedures which are used in order to obtain a reproducible and easily readable EEG recording. These regulations encompass the standards for hardware used for this purpose but also the process of measurement itself.

Before placing the electrodes on the scalp the skin needs to be cleaned from dead cells and other impurities in order to reduce the impedance between the skin and electrodes below 5 kΩ [1]. This is done by light abrasion with a gel made for this purpose in all the areas which will come into contact with electrodes.

Many systems typically use Ag/AgCl electrodes, each of which is attached to an individual wire. Some systems use caps or nets into which electrodes are embedded. This is particularly common when high-density arrays of electrodes are needed. Prior to placing the individual electrode it needs to be covered with a conductive gel or paste, but this step is not necessary if a cap needs to be placed on the patients head. In this case the conductive gel can be injected through the holes in the cap next to the electrodes, made precisely for this purpose. If a cap with dry electrodes is used then there is no need for any skin preparation.

Electrode locations and names are specified by the International 10–20 system, so there wouldn't be any confusion about the electrode placement during the measurements. This system ensures that the naming of electrodes is consistent across laboratories, so it is used in production of EEG caps and must also be followed if using the individual electrodes. The "10" and "20" refer to the fact that the distances between adjacent electrodes are either 10% or 20% of the total front to back or right to left distance of the skull. Each electrode has a letter in its name to identify the lobe and a number to identify the hemisphere location (F-frontal, T-temporal, C-central, P-parietal and O-occipital; "z" refers to an electrode placed on the middle of the scull, even numbers refer to electrode positions on the right hemisphere, whereas odd numbers refer to those on the left hemisphere).

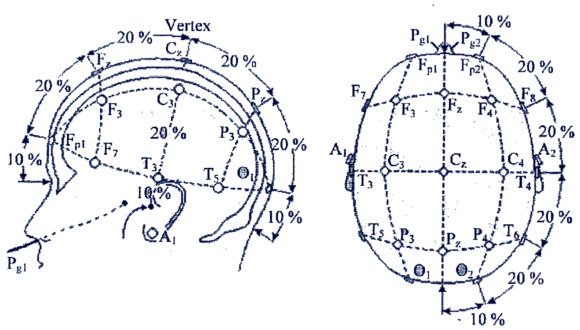

Figure 1.5. Standard 10-20 electrode placement [1]

Most of the time there is no need to use all of the electrodes. The number of channels depends on the purpose of acquisition. In clinics, where various pathologies need to be tested 19 recording electrodes is sufficient (plus ground and system reference) to detect any abnormal activity [11]. However, this number can vary depending on the purpose of EEG recording and the age of a patient. For research purposes the number of electrodes embedded in a cap can go up to above hundred, in which case a map of electrodes must be presented with the results of the study. As opposed to that, if a patient is an infant than the smaller number of electrodes than usual is used due to the relatively small surface available for their placement.

Each electrode is connected to the input of a separate differential amplifier. The measurements are either unipolar or bipolar (Fig 1.6 a) in nature, with most common being the one where reference electrode is connected to the other input of each differential amplifier (Fig 1.6 d).

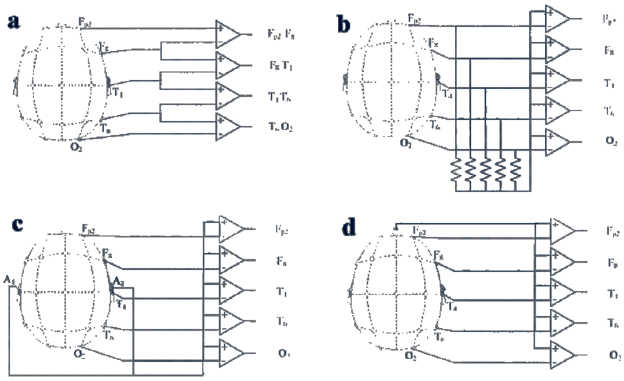

Figure 1.6. Graphical representation of bipolar EEG measurement (a), unipolar with the average signal as reference (b), unipolar with the average of A1 and A2 channel as reference (c) [1] and unipolar with reference electrode placed on the nose (d)

In some cases the average value of A1 and A2 channels can be used as the reference, considering that the EEG activity is minimal in those places (Fig 1.6 c). It is more common though, to connect all channels to 100 kΩ resistor network and acquire their average value and place it as the other amplifier input (Fig 1.6 b) [1].

The amplifiers amplify the voltage between the active electrode and the reference 10^3 to 10^5 times (a typical adult human EEG signal is about 10 µV to 100 µV in amplitude when measured from the scalp). The amplifier must have large CMRR as well as large input impedance that reaches at least 10 MΩ for difference mode input signal and 100 MΩ for the common mode input signal [1].

The amplified signal is passed through an anti-aliasing filter and then sent to a 24bit analog-to-digital converter. Analog-to-digital sampling typically occurs at 256–512 Hz which is more than enough for the purpose of cortical signal measurements. Usually, the digital signal is further filtered with the low pass filter with the higher edge of 70Hz which is sufficient for the purpose of EEG recording.

1.3. EEG signal processing

The EEG signals are normally presented in the time domain. However, many new EEG machines are capable of applying simple signal processing tools such as the Fourier transform to perform frequency analysis and are equipped with some imaging tools to visualize EEG topographies. There have been many algorithms developed so far for processing EEG signals. The operations include, but are not limited to, time-domain analysis, frequency-domain analysis, spatial-domain analysis, and multiway processing.

1.3.1. Brain rhythms

The brain rhythm is the pattern of nerve-cell activity that underlies various behaviors or mental states. As a superposed activity of individual groups of neurons it possesses high enough amplitude to be detected on the scalp. However, one may ask if the interaction between neurons can give rise to oscillations at a different frequency than the firing frequency of individual neurons. Taking into consideration the fact that when the EEG is being recorded the macroscopic brain activity is observed, this does not pose a problem in these measurements, in fact it is encouraged and put to good use at detecting the various mental states.

The first steps in brain wave research were made by Berger himself in 1929. Berger compared the brain waves obtained from subjects with eyes opened and eyes closed. He noticed the increased amplitude in what we today refer to as alpha frequency band while subjects have their eyes closed. Alpha waves are neural oscillations in the frequency range of 8–15 Hz and are dominant during the relaxed mental state, where the patient is at rest or during REM sleep. Since Berger has first recorded and described the origin of these waves, they are also called Berger's waves [3].

Due to his special interest in alpha blockage, Berger has stumbled upon a different type of activity, this one on higher frequencies then alpha waves. They appeared when patients would open their eyes and the alpha activity was replaced by higher amplitudes in 15-25 Hz frequency band. These substitution waves he called the beta activity. Low amplitude beta waves with multiple and varying frequencies Berger associated with active and busy state, or anxious thinking and active concentration. However, nowadays we are also aware that beta waves are associated with the muscle contractions that happen in isotonic movements and are suppressed prior to and during movement changes [3].

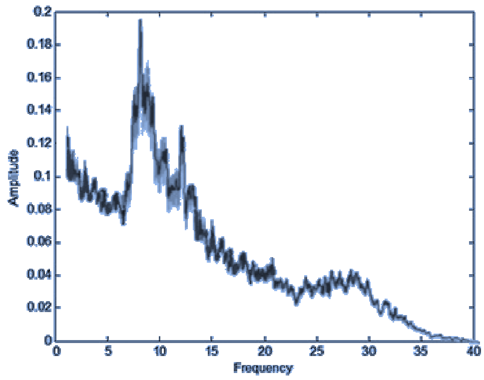

Figure 1.7. EEG spectrum during the resting state shows the prominent peak at 8-12Hz

After a visit to Berger's lab, another scientist came across the idea of creating an improved machine for electroencephalography recordings. In Bristol in the 1930s William Grey Walter made a number of discoveries using his own invention based on the design of Berger's. One of those discoveries included until then unknown delta activity. While Walter demonstrated the use of delta waves to locate brain tumors or lesions responsible for epilepsy, disruptions in these waves are seen in a wide array of disorders. Anomaly in delta activity is seen in adults during states of intoxication or delirium and in those diagnosed with various neurological disorders such as dementia or schizophrenia. In a healthy human it is manifested in early stages of development or during sleep or deep concentration in adulthood [12].

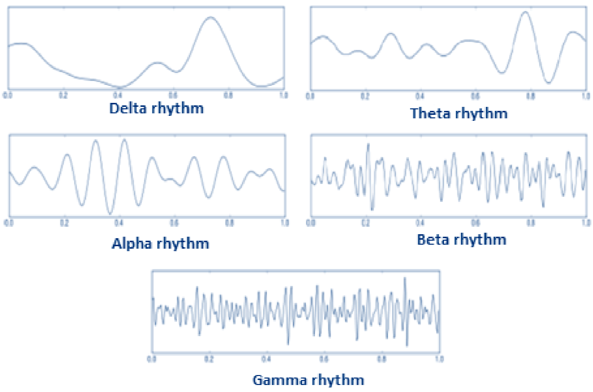

Figure 1.8. Brain rhythms

The discovery of gamma waves had to wait a few decades for the invention of digital EEG, since the gamma band is on frequencies higher than 25 Hz and therefore beyond the possibilities of an analog EEG. It was first described in 1960s, but not much is known about it to this day. It is assumed that this activity is linked to unity of consciousness, performance of complex tasks and high mental functions, such as fear and perception [4].

Unlike the previously described rhythms, theta activity has been difficult to find in humans, even when intracortical electrodes have been available. Ever since the discovery of other rhythms the theta band has been related to oscillations occurring 4 to 7 times per second. These oscillations have only recently been found as a result of cortex neuron activity which can be seen on the EEG. Until 2003 the only known rhythmic activity in that frequency range originated from hippocampus. The hippocampal oscillations were associated with REM sleep and the transition from sleep to waking, and came in brief bursts, usually less than a second long. Even though the cortical theta oscillations had been observed during the transition from sleep and during quiet wakefulness researchers were unable to find any correlation between hippocampal and cortical theta waves [15].

When referring to a group of related activities which cause similar brain wave patterns it is easier to talk about subbands. For example, the subband of the alpha band is mu rhythm, ranging from 8 to 13 Hz. The mu rhythm can be found at the sensorymotor cortex, the part of the brain which controls voluntary movements. Scientists who study neural development are interested in the details of the development of the mu wave in infancy and childhood and its role in learning. There is also evidence that autism spectrum disorder (ASD) can be monitored through these waves. While this is extremely important point, it is not the focus of research revolving around the mu rhythm. In the past two decades scientists have dedicated their time to the development of the brain-computer interface which would allow quadriplegic or patients with ALS to communicate using, among other rhythms, their mu activity.

Even though neural oscillations were observed by researchers as early as Hans Berger their functional role is still not fully understood and there is still a long way to go before brain rhythms can be associated to individual neurons and their roles.

1.3.2. EEG artefacts and their removal

Artefacts occur with any signal measurements, so the EEG is not an exception. Some artefacts are readily distinguished while others so closely resemble cerebral activity that their interpretation is taxing. They can be classified according to their source into two groups: physiological and extraphysiological.

Physiological artefacts originate from the patient himself. They include eye movement, muscle activity (EMG), movement, cardiogenic artefacts and so on.

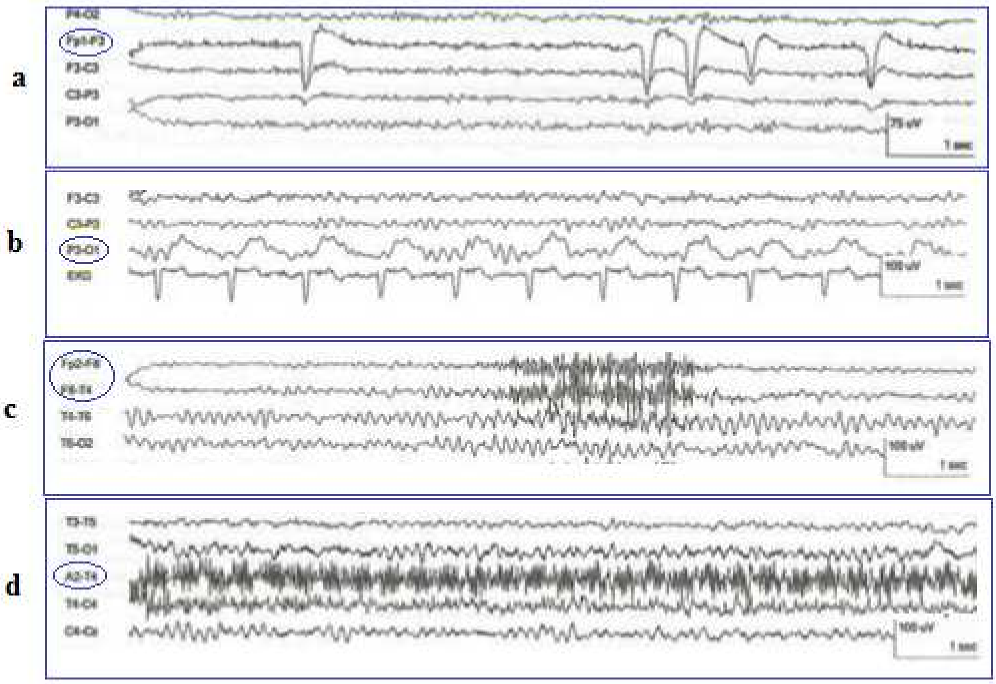

Figure 1.9. EEG artefacts:
eyeblink (a), cardiac (b),muscle (c), 50Hz (d)

The eye artifact is easily distinguishable in the EEG pattern. The most prominent eye-induced artefacts are caused by the potential difference between the cornea and retina, which is quite large compared to cerebral potentials. When the eyes and eyelids are completely still, this dipole does not affect EEG. However, blinks occur several times per minute and the eye movements occur several times per second. Blinks, lateral gaze and slow eye movements can be removed by various filtering methods due to their distinct shapes. One of the easiest ways to remove the EOG from EEG is by recording the electrooculogram along with EEG and then subtracting the previously estimated part of the EOG from the EEG. However, subtracting a linear combination of the recorded EOG from the EEG may not only remove ocular artefacts but also some part of the cerebral activity, since EOG can also be contaminated by EEG. If something like that happens, filtering should be done in a different way, like filtering out high frequency activity from the EOG prior to subtraction.

Cardiogenic artefacts may be removed by simple filtering in frequency domain, since they are distinguishable by their low frequency. The most common type of these artefacts is the result of electrode resting on blood vessel or the result of the movement of head and body with cardiac contractions.

EMG artifact starts as low as 12 Hz and ranges to 300 Hz, so the typical frequency filtering cannot be considered. In addition, while central electrodes can give a relatively pure EEG signal, the others are susceptible to the EMG interference. Muscle activity can best be removed by blind source separation techniques in combination with other processing tools, or using the ICA method (Independent Component Analysis) and then visually reject unsuitable portions of continuous data [2].

The most common extraphysiological artifact is the 50 Hz ambient electrical noise (or 60 Hz, depending on the local power system's frequency), which is quite easy to remove using the notch filter. The example of an EEG signal contaminated with such noise is shown on the Fig. 1.9.

Movement by the patient, or even just settling of the electrodes, may cause electrode pops or spikes originating from a momentary change in the impedance of a given electrode.

1.4. Aims of the master thesis

The subject of this master thesis is a comparative analysis of algorithms for accurate classification of EEG signals in two separate classes, where the left hand movement represents one class and the movement of the right hand the second class. In order to perform the classification, the motor imagery experiment needs to be done in accordance with one of the most efficient paradigms, so the one we implemented in the EEG experiment will be presented in this paper.

For the purposes of better classification, we will construct a visual feedback session using the NXT LEGO Mindstorms robot, so the necessary hardware, software and programming requirements for this task will be explained in the thesis.

Using the signals acquired in high resolution EEG sessions with 96 channels, we classified the EEG signals using the two spatial filtering algorithms. One of these algorithms is the CSP (Common Spatial Pattern) and another is CSSSP (Common Sparse Spatio Spectral Pattern), the latter of which has kept the basic properties of CSP but has the added advantages of spectral filtering.

We will perform the comparative analysis of these two algorithms and describe their advantages and disadvantages. According to this analysis the classification of EEG signals might be improved in relation to time available for the classification as well as the accuracy requirements.

2. BCI

A brain-computer interface provides a direct communication channel between the brain of a subject and a computer, such that mental activities can be used to influence the computer[13]. Nowadays, BCIs are used to enable patients in a late stage of ALS or locked-in syndrome to communicate. Nevertheless, its application does not need to end there. As it is, BCI techniques can be used for the purpose of stroke recovery and lately there has been a widespread initiative to incorporate BCI into the world of entertainment.

2.1. Overview of BCI systems

Like any communication and control system, a BCI has an input, an output, and a translation algorithm that converts the former to the latter. BCI input consists of a particular feature (or features) of brain activity and the methodology used to measure that feature. Each BCI uses a particular algorithm to translate its input (e.g. its chosen EEG features) into output control signals. This algorithm might include linear or nonlinear equations, a neural network, or other methods.

BCI outputs can be cursor movement, letter or icon selection, or another form of device control, and provides the feedback that the user and the BCI can use to adapt in order to optimize communication. As an input BCIs may use frequency-domain (brain rhythms) or time-domain features (slow cortical potentials, P300 potentials, or the action potentials of single cortical neuron). The methodology includes the scalp electrode type and locations, the referencing method, the spatial and temporal filters, and other signal-processing methods used to detect and measure the features [13].

Because BCIs differ greatly in their inputs, translation algorithms, outputs, and other characteristics, they are often difficult to compare. Since some BCIs are commonly used for communication, the measure of their success rate would be the bit rate, the amount of information communicated per unit time. However, it must be taken into consideration that the bit rate depends on both speed and accuracy. Thereby, faster BCI systems naturally have less accurate results and vice versa. Therefore the bit rate is not an entirely objective measure of their performance [13].

BCI can be based on slow cortical signals, oscillations in the alpha and beta range, the P300 evoked potentials or SSVEPs. If the control signal is an imaginary movement of an arm or a leg the BCI input is based on the oscillations in the alpha and beta band. In this case the fluctuation in EEG signal is a result of focusing on the arm or leg movement. P300-potential, which appears in unexpected situations such as a fast change of illumination, can be used in the P300 Speller and similar applications that enable a user to control their environment. The reaction to an unexpected event is used successfully in the detection of one of several options offered on the screen. Each option is randomly illuminated and by focusing on one of those, the user can select it. If the BCI input is in a form of an SSVEP, BCI systems use a visual stimulus, for example a flashing light, which causes the visual evoked potential in the occipital lobe. This evoked potential occurs with the same frequency as the flickering, so if a several options are put before the user, all flickering at different frequencies the system can precisely determine which option the user is observing [4].

Depending on the electrode placement, BCIs can be separated into three groups: invasive, partially invasive and non-invasive BCIs. Invasive BCIs are implanted directly into the grey matter of the brain.

Invasive methods are appropriate only if they are safe and if they provide significant improvement in function over non-invasive methods. At times these criteria can be somewhat blurred by interpretation of significant improvement. There are very few patients who would willingly submit themselves to invasive surgeries necessary in order to implant the electrodes in their cortex. Since the electrodes are placed in the grey matter, invasive devices produce the highest quality signals of BCI devices but are prone to scar-tissue build-up, causing the signal to become weaker in time, or even non-existent, as the body reacts to a foreign object in the brain. The obvious volunteers for this method are patients with severe disabilities, however some people may want to volunteer for research that provides no direct benefit to themselves beyond the knowledge that they are participating in a research project that might help others with similar conditions in the future. Direct brain implants have been used to treat non-congenital (acquired) blindness by implantation onto the patient's visual cortex and creation of phosphenes. Recently, another invasive BCI system was implanted in the cortex of a quadriplegic patient. This system was used to control the robotic hand attached to the patient's wheelchair by imagination of hand movement.

Figure 2.1. Invasive BCI system

Most of the non-invasive implants use EEG cap, and thus produce poor signal resolution because the bone tissue of the cranium deflects and deforms signals, dispersing and blurring the electromagnetic waves created by the neurons. However most patients find them to be preferable to both invasive and partially invasive methods, which defer only in the fact that BCI devices in latter rest outside of grey matter, thus causing less scarring. Noninvasive BCI's use scalp-recorded EEG rhythms or evoked potentials (EP) which is sufficient for a number of purposes, including the motor imagery and P300 experiments, as well as most of EP studies. In this paper the focus will be solely on motor imagery based non-invasive BCIs, since it provides the most convenient EEG signals for testing the relevant EEG processing methods [14].

Figure 2.2. Noninvasive BCI, equipment for P300 speller

2.2. Motor imagery based non-invasive BCIs

Sensory, motor, cognitive and emotional processes can affect the EEG signal by increasing or decreasing the amplitude of cortical rhythms. These fluctuations, as a result of internal or external stimulus are called event related desynchronization or event related synchronization respectively. There is a connection between voluntary/imaginary movements and this phenomenon. Motor imagery, a mental process during which an individual simulates a given action (like hand and foot movement), can modify the neuronal activity in the primary motor cortex area in a very similar way as observable with a real executed movement. Among a small subset of brain states widely considered in the BCI community, lately increasing attention has been devoted to the analysis of EEG signals induced by imagination of motor movement because of its asynchronous and continuous elicitation [16]. During movement the desynchronization in alpha and beta frequency bands occurs. These changes happen in motor cortex prior to, during and after the execution of the movement. Most noticeable changes in the alpha band are the alpha ERD and alpha ERS. Alpha ERD represents a decrease of spectral power in the alpha range right before the movement execution, while the alpha ERS is a subsequent increase in spectral power of alpha band after the motor actions return to the resting state [4].

Motor imagery is a very useful method in many areas. One of the most important is helping people in rehabilitation after cerebrovascular insult. This method is a useful tool in clinical practice, in training and physiotherapy of athletes, in psychology and it already has an application as a basis for controlling devices and various software.

A stroke can be seen as a massive distortion of the capacity of the brain to process neural information, with heterogeneous consequences. Not only the motor system is affected after a stroke, but also the cognitive and emotional systems may be seriously impaired. It is estimated that after acute stroke approximately 80% of the patients have some form of motor impairment. About 20% of these patients regain at least part of their lost motor functions in the subsequent months; thus, of the patients surviving stroke, 50–60% are left with a chronic motor disorder. These disorders are often related to balance, timing and co-ordination, and to loss of strength and/or spasticity in the affected limbs. These motor impairments may substantially compromise quality of life after stroke. However, the treatment of people who have partially or completely lost the use of upper extremities after stroke is not based on healing any possible physical injuries. In the case of complete physical recovery after various traumas most patients remain unable to perform basic movements with ease they possessed preceding pathology. Functional recovery is attributed to reorganization processes in the damaged brain. However, when a functional system is completely damaged, recovery is achieved largely by a process of substitution, for example other brain areas are recruited to take over the functions of the areas damaged by stroke. Therefore, as long as a patient maintains his focus on movements that were once performed without problems neural pathways needed for such actions will not be forgotten. Several studies using brainmapping techniques have found that, during motor imagery, brain areas related to motor execution were activated. The areas that were activated during imagery as well as during the execution of the movement are the prefrontal cortex, the pre-motor cortex, the supplemental motor area, the cingulate cortex, the parietal cortex and the cerebellum [6].

The process of substitution requires patience and constant concentration that most patients in this situation simply do not have. For this reason it is particularly important that during therapy a visual feedback is provided, informing a patient of his success, that would motivate and encourage him to recover faster in some, to him, interesting manner. Keeping this in mind, a variety of games and applications are made which keep patients attention and at the very same time encourage him to practice in the right way.

Every BCI experiment is consisted of certain number of sessions with one subject. In motor imagery experiment each session is further divided into trials. A basic motor imagery experiment subject's task is consisted of maintaining the resting state until a cue is presented to him on the computer screen as a visual stimulus. This event marks the start of one trial. Until then there is a cross on the screen, which is at that moment replaced by an arrow pointing to left or right. In that moment subject follows the instruction given on the screen to the best of his ability by imagining the movement of the right hand (the squeezing motion or finger wriggling) if the arrow is pointing to the right or imagining movement of the left hand in case of the arrow pointing to the left. The visual cue lasts approximately 4 seconds or more, depending on the paradigm, which is when the trial ends. The number of trials can vary with each experiment, and the more trials there are the more accurate the result of the experiment as a whole is.

Here, the matter of subject's involvement and concentration level after a long session should be taken into account when planning the experiment. After a while even the most engrossed subject will gradually loose his focus and the EEG results will no longer be reliable. Between the cues, a subject sees a fixation cross on the screen which signifies the resting period between two trials (cues). The resting intervals should be random and are usually longer than 6 seconds.

During these sessions visual or auditory feedback is sent to the patient informing him of his success. The visual feedback is by far more common and is usually in a form of a bar moving to the left or right, depending on the movement type.

An example of one rehabilitation motor imagery based application would be throwing the ball into the basket located on the left and right side of the screen. Patient's task is to throw the ball into the designated basket in limited time interval which would in this case be the time it takes for the ball to fall, by performing the motor imagery (Fig 2.3). In this way, the patient does not think only about the sensation of movement, but is also trying to succeed in a task that he has been presented with in the most effective way. By achieving the goal of the task the patient is still motivated to play the game and to repeat the same action multiple times, which is necessary for patients who require rehabilitation.

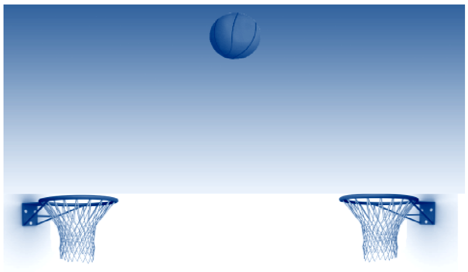

Figure 2.3. One of the games based on motor imagery

In this and many other ways, imagining movements can help patients recover physically as well as improve their everyday life. In addition, similar systems can be used for other games and programs, some of which may even help people with the locked in syndrome in the execution of simpler tasks.

2.3. Disadvantages of non-invasive BCI systems

The high complexity of the human brain and low Signal-to-Noise Ratio (SHR) of EEG signals prevent the BCI systems from decoding every human mental state or intention. EEG signals are noisy and variable over time. Even if the 50 Hz ambient electrical noise is removed, the noise from slight shifts in the position of electrodes remains as a result of changes in the conductance through the skin and interference by hair. As daunting as this problem may sound, most of these interferences can be removed by more or less complex filtering methods, so they will not be further addressed here. True difficulties of BCI systems lie with the experiments themselves as well as within the subjects and patients who execute given tasks.

Since BCI operation depends on the user encoding his or her wishes in the EEG that system measures and translates into output control signals, progress depends on development of improved training methods. The quantity of EEG data available for training is limited, especially if a BCI system must be trained every time an EEG cap is placed on a subject. Even as the subject is performing the same mental task, the recorded electrical activity defers each time he or she places the cap. This may be due to mood changes, subject's concentration, changes in the environment between two sessions or the hardware setup which is slightly different in each session. Some of these issues can be very taxing to address, while others are impossible to influence. Therefore, the focus of improving the prerequisites for acceptable EEG signal should lie with helping the subjects concentrate on the experiment, giving them a clear, achievable goal to increase their motivation and replicating the original conditions of the first session in the following ones. Visual or some other feedback during the sessions can be most helpful in instigating the subject to continue the experiment and try as hard as possible to achieve the goal he was presented with [18].

In most BCI experiments which deal with patients, as opposed to healthy subjects, as well as those developed in the context of gaming, a short setup time is required for a pleasant gaming experience. This implicates that the BCI has to learn user models based on prominent EEG features from a small training set, while the model needs to stay reliable during the whole testing session. The only viable solution to this is the right choice of EEG features used for the purpose of specific BCI system and a variety of temporal and spatial filters used to extract them.

BCI development requires extensive interdisciplinary cooperation, between neuroscientists, engineers, psychologists, programmers, and rehabilitation specialists. With further increases in speed, accuracy, and range of applications, BCI technology could become applicable to larger groups and organizations and could thereby engage the interest of various user populations.

3. HUMANOID ROBOT AS A FEEDBACK IN MOTOR IMAGERY PARADIGM

Accurate EEG feature classification during the motor imagery session largely depends on experiment paradigm and the subject himself. Most of the current research has been focused on the computer side of the BCI such as developing powerful machine-learning algorithms, while less research attention has been given to investigating how BCI users may optimally adapt and help produce better results. It has been shown that visual feedback, not only has a great role in learning a motor skill during the motor imagery session, but also motivates the subject and engages him to further his efforts to achieve the ultimate goal of the session. Thus, it can be said that visual feedback is an important aspect to take into account when designing BCI acquisition sessions. In this chapter the motor imagery paradigm with visual robotic feedback we implemented will be described as well as the experimental setup and utilized hardware and software packages for EEG acquisition.

3.1. The proposed motor imagery paradigm

The proposed EEG experiment with robotic feedback is consisted of two parts: the training and testing session. During the motor imagery training session subjects should be comfortably seated in a chair in a dark room with a blank computer screen placed in front of them. Twenty seconds after the beginning of the session the green fixation cross appears on the black screen. At this point the subjects are in a resting state with hands placed in a relaxed posture comfortably in front of them. After the visual cue, in the form of a red arrow, appears on the screen, the subject is supposed to imagine the movement of the hand corresponding to the direction of an arrow. We suggest this movement to be wriggling fingers as opposed to the simple fist squeezing motion due to its higher complexity. The more complex the movement of the hand the more neurons are activated in the motor cortex, thus producing the more prominent ERD in this area.

During the next 4 seconds, while the cue is shown on the screen subject is required to keep focusing on the feeling and action of a needed hand movement. At the end of the fourth second the blank screen appears again. Until the next time the fixation cross is shown the subject may rest in any way he wishes. The pausing time periods are of various lengths so the subject is always alert. With the reappearance of the fixation cross, and one second later the red arrow, the next trial begins. In the training session we propose to perform at least 20 trials with left hand movement and 20 trials with right hand movement. These trials should be completely random so not to allow a subject to predict the next task.

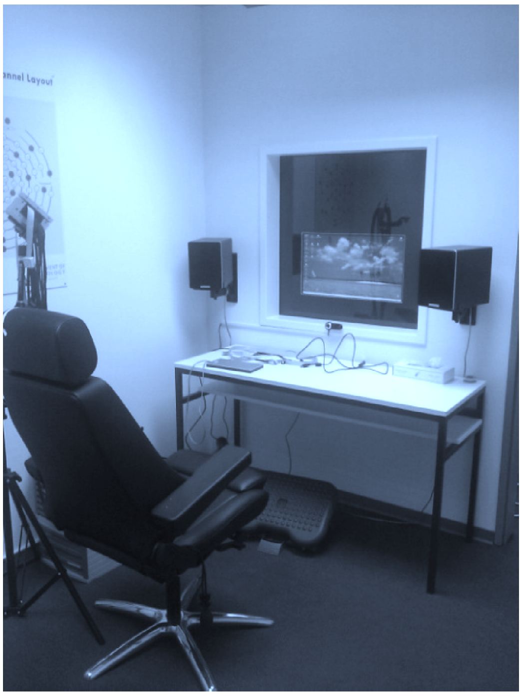

Figure 3.1. The setup and laboratory in which the EEG signals were recorded

While the training session must be done without feedback in a dark room, we suggest that the main part of the experiment is done using the NXT LEGO robot as a visual feedback. The room should be lit just enough for the subject to see the movements of the robot. This feedback is carefully chosen due to its ability to faithfully represent the motor activity. At the beginning of the session the NXT LEGO robot should be placed in front of the subjects, lying on the table, with its head resting closer to the subject.

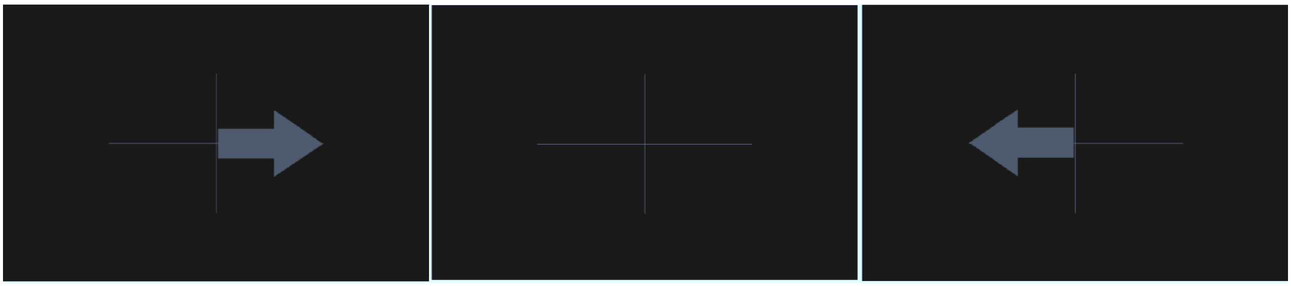

Figure 3.2. Three out of 4 frames shown to the subjects, the fourth remaining frame is a black screen

Prior to the experiment, the robot should be reconstructed to resemble a human being and to move his arms in various speeds. Therefore, by placing it lying down in front of the subject it moves the same hand the subject is imagining the movement of. When the visual cue appears on the screen and the subject imagines the movement of a corresponding hand the recorded EEG signal is being simultaneously processed. Based on the feature extraction from the ongoing signal from the motor cortex and the classification criterion (classifier) trained in between the training and main session the processed trial is classified as a left or right hand imagery. According to this classification the robot's left or right hand, respectively, makes an opening and closing motion in three speeds depending on the classifier output. Therefore, the subject is focused on the imagined hand motion and is, at the same time, watching the same motion be performed by a robot. The EEG signal acquired in this way has a much greater potential for accurate classification than the one from the session without the feedback, or even the one with the moving bar as a feedback.

3.2. LEGO NXT robot

The robot proposed as a visual feedback in this study is LEGO NXT Mindstorms robot. The heart of the Lego Robot is the NXT Intelligent Brick (Fig 3.3) which contains a 32-bit ARM7 microprocessor, four sensor ports (Sensor 1, Sensor 2, and Sensor 3) and three motor ports (A, B, C) [19].

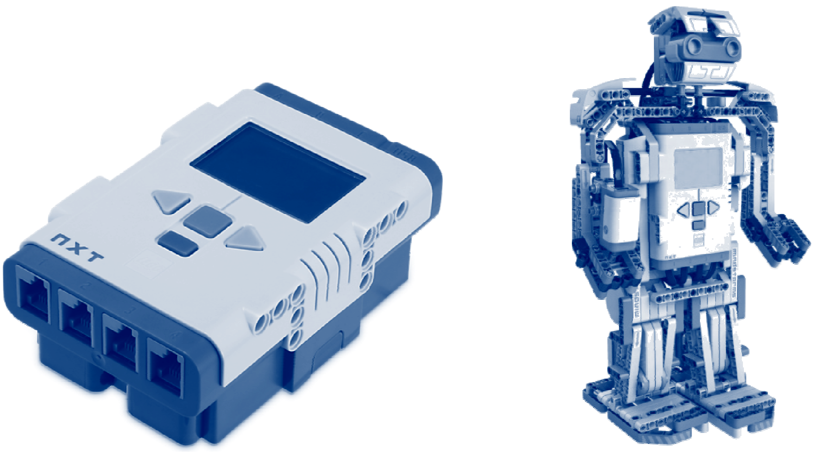

Figure 3.3. The NXT Intelligent Brick (left) and the most common humanoid robot configuration-Alpha Rex (right)

This robot can be assembled in different configurations and can be made to move and sense things through touch and light sensors as it moves. The most beneficial configuration for motor imagery sessions entails the humanoid robot. When assembled it reaches 30 cm in height which is the perfect size for the purpose of visual feedback. The three interactive servo motors and four sensors can be independently controlled by the program created either in NI Labview graphical environment or Matlab programming language by using the appropriate toolbox. It also has a LED display so that messages can be sent to the robot and results and warnings can be displayed.

The robot NXT brick supports Bluetooth wireless communication, so all commands can be transferred wirelessly, which is extremely important considering the robustness of this solution. While working with both patients in clinics and subjects in laboratories it is of utmost importance to reduce the wiring to the minimum so it wouldn't have a negative effect on them, causing the unnecessary level of agitation and distraction. However, as a backup system there is the USB 2.0 port on the NXT brick through which the connection could be established.

The robot can be charged by 1.5 V batteries or lithium rechargeable battery, and both of these can last through two to three motor imagery experiments in average duration of 30 minutes.

Prior to starting the session or making any hardware modifications to the robot, it is wise to establish a wireless connection with computer using the software designated to control the robot during the motor imagery experiment. NI Labview graphical environment would need a driver package which can be downloaded from the manufacturer's website, whereas Matlab needs additional software to be copied on the NXT brick itself as well as the *Fantom driver*. The required file (*MotorControl22.rxe*) is the part of the RWTH toolbox, a Matlab toolbox designed to send information to and from Matlab functions. With the driver installed and the necessary files copied to NXT brick, the wireless connection should be tested. In case everything works properly, the hardware modifications can take place.

For the motor imagery study we did not connect the robot's sensor inputs, since no external sensors are needed for the purpose of the experiment. We used two out of three servo motors and connected them to A and C brick outputs. The servo motor has a built-in rotation sensor that measures speed and rotational distance, and reports back to the NXT Intelligent Brick. This allows precisely measured rotation and complete motor control within one degree of accuracy. We placed these motors as robot's upper arms and are by controlling their rotation we made the hand move in an opening and closing motion. Once the EEG signal is processed the command containing the rotation speed is sent to the NXT brick using the available software and the robot is opening one of the arms in three different speeds we previously programmed.

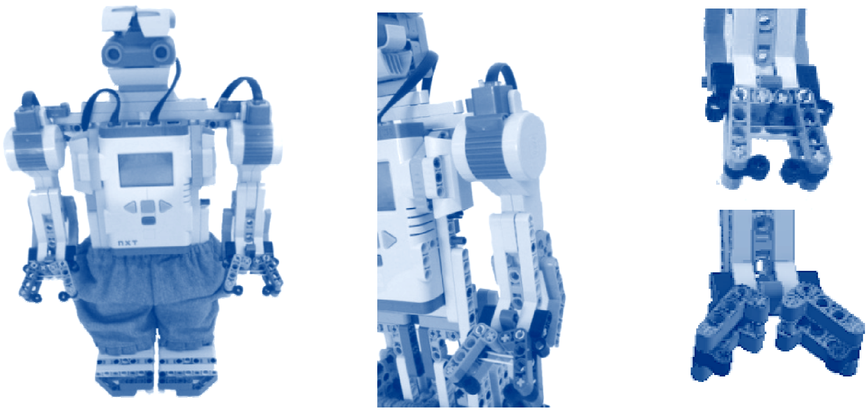

Figure 3.4. The NXT robot prepared for the motor imagery experiment (left) has the built-in motors as his upper arms (middle) which control the hand movement (right)

3.3. Advantages and disadvantages of robotic visual feedback

The LEGO NXT robot as a visual feedback encourages the subject to either keep performing the task without making any changes to his motor imagery strategy in case of correct robot response, or increase his focus and perhaps change the tactics in order to correct the opposite action of the robot.

This kind of visual stimulus is preferable to a moving bar since it imitates the exact movement the patient is supposed to imagine. The idea of using the movement of NXT robot's hands, however, was not the part of original paradigm. At first, our goal was to program the robot to walk forward and backward in the subject's line of vision. However, we abandoned this approach partially due to encountering the same problem as with the moving bar. While watching the bar or the robot move left or right, the subjects switch their focus to those events, and for a very short but sufficient period of time, they no longer perform the motor imagery task. Instead they will the bar to move using other inefficient mental strategies. Therefore, the bar no longer moves in accordance to subjects' wishes and eventually they return to the original strategy.

This problem can be avoided by extensive motor imagery training. However, most subjects do the experiment only once without the benefit of previous experience. Making the feedback the same type of movement as the imagined task would immensely help the subject to maintain their focus. This way, the subject no longer tries to substitute the original strategy, since they do not receive the visual stimulus which defers from their task.

NXT robot has a role of an immediate visual feedback of performance, so we also considered the influence of the visual feedback on motor cortex. There has been some evidence that a rich visual representation of the feedback signal (for example in the form of a 3-dimensional video game or virtual reality environment, and therefore also the humanoid robot's movement) may enhance the learning progress in a BCI task [6]. In particular, the mentioned studies suggest employing rather realistic and engaging feedback scenarios, which are closely related to the specific target application. Another important point to consider is the interference of a response from the realistic feedback stimulus with the mental motor imagery task. In some cases, this may impair the processing and subsequent EEG control. Oscillations in the mu and beta frequency bands are reactive to both motor imagery and observation of biological movement [27]. Therefore, it is not unlikely that a realistic feedback presentation may interfere with the motor imagery related brain signals used in the experiment. There is evidence from functional magnetic resonance imaging (fMRI) studies that this kind of action observation is associated with activation of premotor cortical structures [12].

There is one other issue with the LEGO NXT Mindstorms robot which can be considered as both advantage and disadvantage. While its motors are very powerful, the level of noise they create can be somewhat distracting for the subject. Even if the noise cannot be avoided, we turned this seemingly insurmountable obstacle into advantage. Since the motor for the right hand is located on robots right side and motor for the left hand on robot's left side the noise can be observed as an audio feedback. The sound level on subject's left side will be higher if robot makes the left hand grasp as opposed to the right hand grasp and vice versa. By presenting the subjects with a visual feedback they are aware of and paying attention to and an auditory one which subconsciously tells them if their task was done correctly, their performance can potentially be drastically improved.

3.4. Acquisition and processing software

The motor imagery experiment described in this thesis consists of two parts: the training and the feedback session. During the acquisition in the training session the complex processing methods with spatial or spectral filtering were not used. Instead the signals, acquired using the EEG cap and amplifiers, are simply written into a file awaiting further analysis. After this first session, signals require further processing and feature vector extraction before the classifier for the next (feedback) session can be trained. Only when the classifier is trained the feedback session can be initiated. Signals acquired from the session with feedback can be considered optimal for the later use in testing various more complex filtering and classification options as the CSP and CSSSP.

3.4.1. OpenViBE software

The optimal acquisition software for motor imagery experiments with feedback is the OpenViBE Acquisition Server combined with OpenViBE Designer 0.14.0.

OpenViBE Acquisition Server is a tool designed to communicate with hardware signal acquisition devices and forward acquired signals and other experiment information to OpenViBE applications in a way compliant with the OpenViBE format specification. The acquisition server does not communicate directly with acquisition devices. Instead, it provides the user with a set of drivers to choose from, each one being dedicated to a given device model (Fig 3.5).

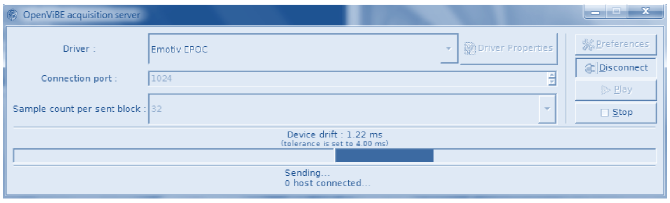

Figure 3.5. Graphical user interface for OpenViBE acquisition software

OpenViBE Designer relies on a graphical user interface to provide the user with signal processing tools in an intuitive way. It serves to create and execute a scenario, an application which may contain all parts of the session in the form of algorithm boxes. The algorithm boxes present the built in signal acquisition, processing, visualization and presentation tools which may be arranged in various order to form any BCI scenario [20].

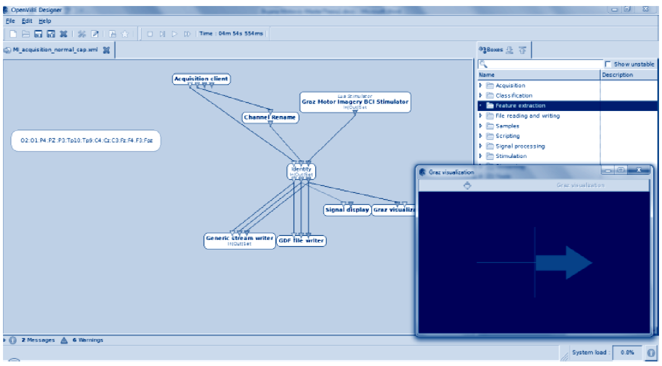

Figure 3.6. Graphical user interface for OpenViBE designer.
The motor imagery scenario is running with the cue presentation in separate window.

The main part of any scenario involving the signal acquisition is an Acquisition Box, followed by necessary processing boxes. The visualization tools are not obligatory, but in the case of BCI models are highly recommended.

For the purposes of motor imagery session another unavoidable algorithm box we used is the *Graz Motor Imagery BCI Stimulator*. While this toolbox requires the script in Lua programming language to function it is still the fastest and most productive way of executing the scenario with or without a graphical motor imagery feedback. By specifying the exact duration of the resting, cue and feedback period and by programming the order of operations in Lua, this box creates the scenario of the whole motor imagery experiment and once it is executed it loads necessary labels which mark the onset points of all events in the experiment. These labels are joined to the acquired signal, providing the necessary experiment information for accurate subsequent processing.

Since two motor imagery sessions are required, one without and the other with robotic feedback, we used two separate OpenViBE scenarios. In addition, the classifier needs to be trained in between these sessions, so using the OpenViBE processing tools for this purpose can be extremely beneficial. Therefore, in order to obtain the high quality EEG three OpenViBE scenarios in total should be used.

The first scenario was designed so it could receive the signals from the amplifiers and save them in the predetermined OV (OpenViBE) file. By initiating this scenario a training session starts. The *Graz Motor Imagery BCI Stimulator* was employed in order to present the visual stimulus in the form of left and right arrows to a subject and to place markers in signals at appropriate time points, like the start of the session, the onset of a visual cue or its disappearance and at the beginning of other significant events. The reason the OpenViBE is one of the leading software in this field, is the marker placement without any delays, which is extremely important in EEG recordings due to very fast amplitude and frequency changes.

The second scenario, as was already mentioned, does not involve EEG acquisition. Instead it loads the data saved in the OV file during the training session and uses the simple processing tools to train a classifier. Processing tools are applied in the form of OpenViBE algorithm boxes, making the whole scenario less time consuming for the programmer. However, not all of the data from the OV file is used in the classifier training; only two, most important channels according to the previous motor imagery studies have been chosen, the C3 and C4 channels. Data from these two channels was bandpass filtered in 8 to 24 Hz frequency range. Afterwards, based on the markers from the *Graz Motor Imagery BCI Stimulator* in the training sessions, the trials for left and right hand motor imagery were separated and features for each of them extracted using the following criterion:

$$f_{v_y} = \log(1 + \frac{\sum_{i=1}^{n} x_{y,i}^2}{n}) \tag{1}$$

where fv_y stands for the feature vector of y class, y belonging to left or right hand trials, x_{yi} is a sample i of the trial of class y and n is the number of samples in the trial. By loading these feature vectors for all trials in the *Classifier trainer*, another OpenViBE algorithm box, the classifier based on Linear Discriminant Analysis (LDA) is trained and ready to use in the session with visual feedback.

The third scenario is reserved for the feedback session. Before the start of the session the classifier trained in the previous scenario should be loaded. Once started, the scenario opens a new window with visual cues, much like in the first scenario. It initiates the signal acquisition and saves raw, unprocessed signals in a predetermined OV file. The only difference is that this time the subject has a visual feedback in a form of a robot. For the feedback to be effective the minimal amount of signal processing is needed in OpenViBE. The first step is, as in the classifier training, the bandpass filtering in alpha and beta range (8-24 Hz) of relevant channels (C3 and C4). By using the same feature extraction algorithm over the short intervals they are sorted into appropriate classes according to the trained LDA classifier. The output of the classifier algorithm box reflects the classification algorithm status in the form of a matrix of value. The LDA classifier sends the hyperplane distance as its status, where the two separate planes signify the left and right hand imagery. However, these outputs need to be translated into visual feedback by controlling the robot's motors. Due to OpenViBE's lack of NXT drivers and resulting inability to establish a bluetooth connection to the NXT brick, this part of the feedback session must be taken over by some other program which can communicate with the OpenViBE.

The only two programs capable of controlling the NXT brick are NI Labview graphical environment and Matlab programming language, but only the latter can also freely exchange data with OpenViBE. Therefore, we found that the optimal choice is to incorporate a Matlab Script into OpenVibe using the *Matlab scripting box*. The *Matlab Scripting box* uses the Matlab Engine to process data using Matlab. This box is currently compatible only with Matlab 32 bits on Windows operating system and its role is to call a previously written Matlab functions and execute them, using the input arguments from the OpenViBE.

We additionally configured the Matlab Scripting box by specifying the clock frequency which indicates how many times per second the box will be called from the OpenViBE. The input arguments, other than data which needs to be forwarded to Matlab, include three Matlab functions which will be called from the OpenViBE. We constructed these functions so they could communicate with OpenViBE in the following way: *Initialize function* is called only once during the scenario, when the first call to Matlab is requested; *Process function* is executed in accordance with the Matlab clock frequency, while the *Uninitialize function* is called when the Matlab scripting no longer needs to be executed.

This is where the OpenViBE's part in the experiment ends and the process of sending the information to NXT brick is taken over by Matlab and the specifically designed RWTH Matlab toolbox with appropriate NXT drivers.

3.4.2. Matlab RWTH toolbox

The RWTH Matlab toolbox is developed to control LEGO NXT Mindstorms robots with Matlab via a wireless Bluetooth connection or via USB. This software is a free open source product designed by the Aachen University. The LEGO Mindstorms NXT Bluetooth Communication Protocol allows this remote control concept to be a fully functional counterpart and equal rival to NI Labview graphical environment, the original software for the control of the LEGO robot. This toolbox enables combining the robot applications with complex mathematical operations, digital signal processing and visualizations within MATLAB**.**

The data sent form the OpenViBE is in the form of an array, signifying the command which needs to be sent to the robot. One element of an array holds the numerical information on the hyperplane distance for one time period. Larger distance means the higher probability of correct classification of that period, which is the direct consequence of relevant cortex region activation in a subject. The difference between the hyperplane distances for the two classes is marked by using the positive numbers for one class and negative numbers for the other class.

We designed the Matlab *Initialize function* to establish the bluetooth connection to the robot using the RWTH toolbox functions. Once the robot is connected this step does not repeat with each call to the Matlab Scripting Box. Every following call to the Matlab scripting box starts the Process function. Depending on the imported hyperplane distance six types of commands are sent from the Matlab *Process function*. Three of these we reserved for the three levels of rotation power used to continuously perform the left hand squeezing motion and three levels to perform the right hand squeezing motion in robot. The greater the hyperplane distance of a right/left hand motor imagery, the faster the robot's right/left hand will move. When the session has ended with the last call to the

Matlab Scripting box, the command is sent through the *Uninitialize function* to the robot to terminate a bluetooth connection and the experiment ends.

The data recorded in the feedback session by the OpenViBE acquisition software and OpenViBE designer is unprocessed data of greater quality due to the realistic feedback which improves the discrimination between the activated cortex regions of the left and right brain hemisphere and therefore can be used with higher success rate in spatio-spectral analysis.

3.5. Possible hardware and software inconsistencies

One of the most noticeable problems we encountered while running the proposed setup comes in the form of hardware and software inconsistencies. Therefore, there are several important issues which should be kept in mind when planning the motor imagery experiment with NXT LEGO Mindstorms robot as a feedback.

The first problem involves software compatibility. OpenViBE software is compatible only with 32bit systems and does not offer full support for 64bit. While other OpenViBE boxes may run on both architectures, the *Matlab scripting box* cannot. Therefore it is of vital importance to do all the recordings on the system architecture recommended by the publisher.

Furthermore, the RWTH software has its own limitations, making it possible to run only under Matlab version 2012b or higher. In addition, it must be taken into account that OpenViBE only establishes connection with 32bit Matlab versions.

One of the main issues with this system is that the bluetooth device used for connection must be v 1.2 compliant and must have a Cambridge chipset. If one of these options is not satisfied, the connection will not be established.

Even if these setbacks are sometimes time consuming to fix, one must keep in mind all the advantages and possibilities which come with a robotic feedback system. However, with the right hardware and by following the manufacturer's instructions there should be no problem in running this motor imagery session.

4. SPATIAL AND SPATIO-SPECTRAL FILTERING FOR EEG MOTOR IMAGERY CLASSIFICATION

In this chapter the spatial and spatio-spectral filtering by means of the Common Spatial Pattern filters will be discussed. We will explain the CSP and CSSSP algorithm, their mathematical background and application in motor imagery classification. The advantages and disadvantages of CSP will be explained as well as our Matlab implementation of both algorithms applied for the purposes of this thesis.

4.1. Common Spatial Pattern

Extracting subject-specific discriminative patterns from high-dimensional spatio-temporal EEG signals primarily requires some form of spatial filtering. In this thesis we applied the spatial filtering to 96-channel EEG recordings obtained during right and left hand motor imagery. With respect to the topographic patterns of brain rhythm modulations, the Common Spatial Pattern algorithm has proven to be very useful for motor imagery BCI.

This method was first introduced as a decomposition method which finds projections common to two states of brain activity and afterwards successfully applied to the classification problem of the two states. The original problem formulation was based on classification of normal and abnormal brain states, since the purpose of the algorithm was pathology detection. Classification by a human being is usually based on a small number of features such as the peak value or fundamental frequency. Each of these measurements carries significant information for classification and is selected according to the physical meaning of the problem [21]. Obviously, as the number of inputs to a classifier becomes smaller, the design of the classifier becomes simpler. In order to enjoy this advantage, there has to be some way to select or extract important features from the observed samples. This problem is called feature extraction. Feature selection can be considered as a mapping from the n-dimensional space to a lower-dimensional feature space. The simplest classification method uses two distinctive feature vectors which could be represented in two-dimensional space. An example of two distributions corresponding to normal and abnormal conditions, where points depict the locations of samples and solid lines are the contour lines of the probability density functions is shown on Fig 4.1.

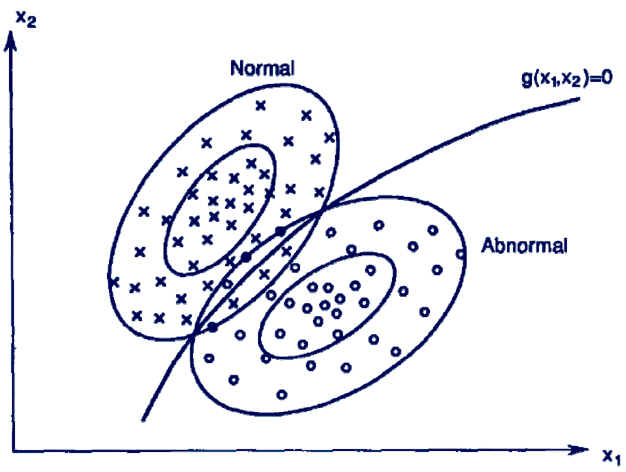

Figure 4.1. Distribution of samples from normal and abnormal states [21]

If we know these two distributions $X \in (x_1 \cup x_2)$ from past experience, we can set up a boundary $g(x_1, x_2) = 0$ between them which divides the two dimensional space into two regions. Once the boundary is selected, we can classify a sample without a class label to a normal or abnormal state, depending on $g(x_1, x_2) > 0$ or $g(x_1, x_2) < 0$. We call $g(x_1, x_2)$ a discriminant function, and a network which detects its sign is called a pattern recognition network or a classifier [21].

The CSP method is based on a decomposition of the raw EEG signals into spatial patterns, which are extracted from two populations of single trial EEG. These patterns are meant to maximize the difference between these populations. When processing data from the motor imagery experiment one population consists of EEG recordings during left hand motor imagery and the other population consists of right hand motor imagery data [22].

Motor imagination can be captured through spatially localized band-power modulation in mu and beta rhythms. The frequency band, on which the CSP algorithm operates, can be selected either manually or set to a broad band filter. The manual selection is preferable in the feedback session, when the prior information about the specific subject's EEG rhythms is available from the training session, while during the training itself it is near impossible to determine the optimal mu band in a new subject. For this reason, for the analysis of the CSP algorithm, the broad band filter will be used (7-30 Hz) in further proceedings.

If the EEG is first preprocessed in order to focus on the mu and beta band, then a signal projected by a spatial filter focusing on the left-hand area is characterized by a strong motor rhythm during the imagination of right-hand movements, and by an attenuated motor rhythm if movement of the left hand is imagined. This can be seen as a simplified exemplary solution of the optimization criterion of the CSP algorithm: maximizing variance for the class of right-hand trials and at the same time minimizing variance for left-hand trials.

Let us denote the CSP filter by:

$$\boldsymbol{Z_i} = \boldsymbol{\omega}^{\mathrm{T}} \boldsymbol{s_i} \tag{2}$$

where $\boldsymbol{\omega} \in \mathbb{R}^{chxd}$ is a spatial filter matrix, $\boldsymbol{Z_i} \in \mathbb{R}^{dxt}$ a filtered signal matrix for *i*-th trial and $\boldsymbol{s_i} \in \mathbb{R}^{chxt}$ a bandpassed EEG signal matrix for *i*-th trial (*ch* stands for the number of EEG channels used for the acquisition, *t* is a duration of one trial given in samples and $d := (2i | i \in \mathbb{N})$ is a dimension of a filter solution). Therefore, the spatial filter $\boldsymbol{\omega}$ projects EEG trials to the signal $\boldsymbol{Z}$ with minimum two channels. As was already mentioned, the idea of CSP is to find a spatial filter such that the projected signal has high power for one class and low power for the other. If *d*=2 then each row of the projection matrix gives the information about one class probability for the trial in question.

Using the following notation the composite spatial covariance matrix $\boldsymbol{\Sigma_l}$ of the EEG is given as:

$$\boldsymbol{\Sigma_l} = \frac{1}{n_l} \sum_{i=1}^{n_l} \frac{\boldsymbol{s_i} \boldsymbol{s_i}^{\mathrm{T}}}{trace(\boldsymbol{s_i} \boldsymbol{s_i}^{\mathrm{T}})} \tag{3}$$

where *i* stands for one of the total n_l trials in class $l \in$ [class1,class2].

The CSP analysis is based on calculating a matrix $\boldsymbol{\omega}$ and diagonal matrix $\boldsymbol{D}$ with elements in [0,1] such that:

$$\boldsymbol{\omega} \boldsymbol{\Sigma_1} \boldsymbol{\omega}^{\mathrm{T}} = \boldsymbol{D} \tag{4}$$

and

$$\boldsymbol{\omega}\boldsymbol{\Sigma}_2\boldsymbol{\omega}^{\mathrm{T}} = \boldsymbol{I} - \boldsymbol{D}. \tag{5}$$

According to the (2) and (3) the problem can be formulated in the following way: the goal of the CSP is finding the spatial filter such that the sum of variances of the filtered signal is maximized for one class and minimized for another. Eventually, the formulation of this problem can be expressed as the following optimization problem:

$$\max_{\boldsymbol{\omega}} \sum_{i=1}^{n_1} \mathrm{var}(\boldsymbol{\omega}^{\mathrm{T}}\boldsymbol{s_i}) \text{ , so that } \sum_i \mathrm{var}(\boldsymbol{\omega}^{\mathrm{T}}\boldsymbol{s_i}) = 1 \tag{6}$$

$$\min_{\boldsymbol{\omega}} \sum_{i=1}^{n_2} \mathrm{var}(\boldsymbol{\omega}^{\mathrm{T}}\boldsymbol{s_i}) \text{ , so that } \sum_i \mathrm{var}(\boldsymbol{\omega}^{\mathrm{T}}\boldsymbol{s_i}) = 0 \tag{7}$$

where *var* is the variance of the vector. Using the definition of the variance we simplify the problem to:

$$\max_{\boldsymbol{\omega}} \boldsymbol{\omega}^{\mathrm{T}}\boldsymbol{\Sigma_1}\boldsymbol{\omega} \text{ , so that } \boldsymbol{\omega}^{\mathrm{T}}(\boldsymbol{\Sigma_1} + \boldsymbol{\Sigma_2})\boldsymbol{\omega} = 1 \tag{8}$$

In order to calculate $\boldsymbol{\omega}$, first the whitening transformation has to be done over the matrix $\boldsymbol{\Sigma_1} + \boldsymbol{\Sigma_2}$. This means it is necessary to determine the matrix $\boldsymbol{P}$ such that:

$$\boldsymbol{P}(\boldsymbol{\Sigma_1} + \boldsymbol{\Sigma_2})\boldsymbol{P}^{\mathrm{T}} = \boldsymbol{I} \tag{9}$$

The whitening transformation equalizes the variances in the space, so that all eigenvalues of $\boldsymbol{P}(\boldsymbol{\Sigma_1} + \boldsymbol{\Sigma_2})\boldsymbol{P}^T$ are equal to one. This decomposition can always be found due to the positive definiteness of $\boldsymbol{\Sigma_1} + \boldsymbol{\Sigma_2}$. If $\boldsymbol{\Sigma_1}$and $\boldsymbol{\Sigma_2}$are transformed as

$$\boldsymbol{S_1} = \boldsymbol{P}\boldsymbol{\Sigma_1}\boldsymbol{P}^{\mathrm{T}} \tag{10}$$

$$\boldsymbol{S_2} = \boldsymbol{P}\boldsymbol{\Sigma_2}\boldsymbol{P}^{\mathrm{T}} \tag{11}$$

then $\boldsymbol{S_1}$ and $\boldsymbol{S_2}$ share common eigenvectors. Due to this fact it is relatively easy to calculate an orthogonal matrix $\boldsymbol{B}$ and a diagonal matrix of eigenvalues $\boldsymbol{D}$ from (2) and (3) by spectral theory such that

$$\boldsymbol{S_1}^{\mathrm{T}} = \boldsymbol{B}\boldsymbol{D}\boldsymbol{B}^{\mathrm{T}} \tag{12}$$

From $\boldsymbol{S_1}+ \boldsymbol{S_2}=\boldsymbol{I}$ it follows that:

$$\boldsymbol{S_2}^{\mathrm{T}} = \boldsymbol{B}(\boldsymbol{I} - \boldsymbol{D})\boldsymbol{B}^{\mathrm{T}} \tag{13}$$

The eigenvector with largest eigenvalue for $\boldsymbol{S_1}$ has the smallest eigenvalue for $\boldsymbol{S_2}$ and vice versa. This property makes the eigenvectors $\boldsymbol{B}$ useful for classification of the two distributions. The projection of whitened EEG onto the first and last eigenvectors in $\boldsymbol{B}$ will give feature vectors that are optimal for discriminating two populations of EEG. The final decomposition that satisfies (2) and (3) can be obtained from:

$$\boldsymbol{\omega} = (\boldsymbol{B}^{\mathrm{T}}\boldsymbol{P})^{\mathrm{T}} \tag{14}$$

The interpretation of $\boldsymbol{\omega}$ is twofold, the rows of $\boldsymbol{\omega}$ are the stationary spatial filters, whereas the columns of $\boldsymbol{\omega}^{-1}$ can be seen as the CSPs or the time-invariant EEG source distribution vectors. The decomposition (mapping) of a trial $\boldsymbol{s_i}$ is given by (1).

The further classification is based on feature vector extraction. The rows of the $\boldsymbol{Z_i}$ maximize the difference of variance of left versus right hand imagery. Various algorithms can be used for the extraction of feature vectors. In the analysis for the purpose of this thesis, we applied one of the most common:

$$f_{v_y} = \log(1 + \frac{\sum_{i=1}^{t} \boldsymbol{Z}_{y,i}^2}{t}) \tag{15}$$

The feature vectors of left and right trials are further used to calculate a linear classifier (based on the LDA).

4.2. Combined spectral and spatial filter

Many research groups have devoted their efforts to either the frequency band selection or optimal spatial filters learning via the Common Spatial Pattern (CSP) algorithm. However, since the spectral filtering and the spatial filtering are generally operated in order in a motor imagery classification system, the optimization of the spatial filters and the spectral filters should be considered simultaneously in a unified framework.

The idea of a combined spectral and spatial filter has been the subject of many papers and studies during the past five years. Only recently has been developed a spatio-spectral filter good enough for the BCI techniques. One of the most efficient filters was created by Lemm [22], and it was an extension of CSP filter. The Common Spatio-Spectral Pattern (CSSP) can be regarded as a CSP method with the time delay embedding. After that, the new algorithm immerged, the Common Sparse Spatio Spectral Pattern (CSSSP). This algorithm is to learn a complete global spatio-temporal filter in the spirit of CSP and CSSP.

4.2.1. Common Spatio-Spectral Pattern (CSSP)

The CSSP method is based on the concept of deterministic low-dimensional chaos. Mathematically, the system in deterministic state is defined by a first order differential equation in a state space $\Gamma \subset \mathbb{R}^{D}$. Such system therefore possesses D natural variables, but the measurement is usually a nonlinear projection onto a scalar value. Therefore, it is necessary to reconstruct an equivalent of the state space Γ with all its dimensions using the time delay embedding method [23].

Given $\boldsymbol{s_i}$, the signal $\boldsymbol{s_i^\tau}$ is defined to be the signal delayed by τ timepoints with respect to the sampling rate. In CSSP, the usual CSP approach is applied to the concatenation of $\boldsymbol{s_i}$ and $\boldsymbol{s_i^\tau}$ in the channel dimension and the delayed signals are treated as new channels. While it is possible to add several delayed channels, thus increasing the complexity of the filter itself, in this paper the method will be explained on the example of one added channel.

$$\boldsymbol{Z_i} = \boldsymbol{\omega_0}^{\mathrm{T}} \boldsymbol{s_i} + \boldsymbol{\omega_\tau}^{\mathrm{T}} \delta_\tau \boldsymbol{s_i} \tag{16}$$

By this concatenation step the algorithm is able to neglect or emphasize specific frequency bands. In order to use the previous equations given in CSP the representation of appended delayed vectors $\delta_\tau \boldsymbol{s_i}$ is:

$$\boldsymbol{s_i^{new}} = \begin{bmatrix} \boldsymbol{s_i} \\ \delta_\tau \boldsymbol{s_i} \end{bmatrix} \tag{17}$$

The optimization criterion can be formulated according to (6) and (7) using the class covariance matrices obtained from $\boldsymbol{s_i^{new}}$**.** The difference in the solution will of course be noticeable in the spatial pattern matrix $\boldsymbol{\omega^{new}}$ whose columns divide in two submatrices: $\boldsymbol{\omega_0}$ that applies to $\boldsymbol{s_i}$ and $\boldsymbol{\omega_\tau}$ that applies to the delayed channels $\delta_\tau \boldsymbol{s_i}$. The decomposition into $\boldsymbol{Z_i}$ can be done in the following way:

$$\boldsymbol{Z_i} = \sum_{c=1}^{ch} \boldsymbol{\omega_{0_c}}^{\mathrm{T}} \boldsymbol{s_{i_c}} + \boldsymbol{\omega_{\tau_c}}^{\mathrm{T}} \delta_\tau \boldsymbol{s_{i_c}} \tag{18}$$

where *ch* is a number of EEG electrodes. This expression can further be transformed to resemble a finite impulse response (FIR) filter:

$$\boldsymbol{Z_i} = \sum_{c=1}^{ch} \gamma_c \left(\frac{\boldsymbol{\omega_{0_c}}^{\mathrm{T}}}{\gamma_c} \boldsymbol{s_{i_c}} + \frac{\boldsymbol{\omega_{\tau_c}}^{\mathrm{T}}}{\gamma_c} \delta_\tau \boldsymbol{s_{i_c}} \right) \tag{19}$$

where γ_c is a pure spatial filter. The coefficients in the brackets represent a FIR filter for each electrode *c*. By adjusting γ_c and a decomposition matrix a fine tuning of the overall frequency filters, e.g., an adaptation to the spectral EEG peaks is possible.

4.2.2. Common Sparse Spatio Spectral Pattern (CSSSP)

The Common Sparse Spatio Spectral Pattern (CSSSP) filter is a further extension of the CSSP [24]. The CSSSP's digital frequency filter is also restricted to FIR and is given by:

$$y(t) = \boldsymbol{b}(1)x(t) + \boldsymbol{b}(2)x(t-1) + \cdots + \boldsymbol{b}(n_b)x(t - n_b - 1) \tag{20}$$

Furthermore, the coefficient $\boldsymbol{b}(1)$ is defined to the value 1 and the length of $\boldsymbol{b}$ is fixed to some T>1 to avoid overfitting. The optimization problem in CSSSP can be defined as looking for a real valued sequence $\boldsymbol{b}$ with $\boldsymbol{b}(1)=1$ such that the trials

$$\boldsymbol{s_{i,b}} = \boldsymbol{s_i} + \sum_{\tau=2}^{T} b_\tau \boldsymbol{s_i^\tau} \tag{21}$$

can be classified with greater accuracy than with CSSP. The optimization problem is inherited from the CSP, relying on (6) and (7) with the only difference being that the bandpassed signal $\boldsymbol{s_i}$ is replaced by the signal containing the FIR filter $\boldsymbol{s_{i,b}}$.

$$\max_{\boldsymbol{\omega},\boldsymbol{b}} \sum_{i=1}^{n_1} \mathrm{var}(\boldsymbol{\omega}^{\mathrm{T}} \boldsymbol{s}_{i,\boldsymbol{b}}) \text{ , so that } \sum_i \mathrm{var}\left(\boldsymbol{\omega}^{\mathrm{T}} \boldsymbol{s}_{i,\boldsymbol{b}}\right) = 1 \tag{22}$$

$$\min_{\boldsymbol{\omega},\boldsymbol{b}} \sum_{i=1}^{n_2} \mathrm{var}(\boldsymbol{\omega}^{\mathrm{T}} \boldsymbol{s}_{i,\boldsymbol{b}}) \text{ , so that } \sum_i \mathrm{var}\left(\boldsymbol{\omega}^{\mathrm{T}} \boldsymbol{s}_{i,\boldsymbol{b}}\right) = 0 \tag{23}$$

In order to better define the optimization problem the covariance matrices for both classes are needed. However, due to the presence of delayed channels the covariance matrices can not be as simple as in CSP. In CSSSP the covariance matrices are defined as:

$$\boldsymbol{\Sigma}_{\boldsymbol{y}}^{\boldsymbol{\tau}} := E\left(\langle \boldsymbol{s}_{\boldsymbol{i}}(\boldsymbol{s}_{\boldsymbol{i}}^{\boldsymbol{\tau}})^{\mathrm{T}} + \boldsymbol{s}_{\boldsymbol{i}}^{\boldsymbol{\tau}} \boldsymbol{s}_{\boldsymbol{i}}^{\mathrm{T}} \rangle \mid i\!: Trial\ in\ Class\ y\right) \quad \text{for } \tau > 0 \tag{24}$$

$$\boldsymbol{\Sigma}_{\boldsymbol{y}}^{\boldsymbol{0}} := E\left(\langle \boldsymbol{s}_{\boldsymbol{i}} \boldsymbol{s}_{\boldsymbol{i}}^{\mathrm{T}} \rangle \mid i\!: Trial\ in\ Class\ y\right) \quad \text{for } \tau = 0 \tag{25}$$

The problems defined by (22) and (23) can be approximately simplified using the correlation between the signal and by τ delayed signal.

$$\max_{b} \max_{\omega} \boldsymbol{\omega}^{\mathrm{T}} \left(\sum_{\tau=0}^{T-1} \left(\sum_{j=1}^{T-\tau} \boldsymbol{b}(j) \boldsymbol{b}(j+\tau) \right) \boldsymbol{\Sigma}_{\boldsymbol{1}}^{\boldsymbol{\tau}} \right) \boldsymbol{\omega} \tag{26}$$

so that

$$\boldsymbol{\omega}^{\mathrm{T}} \left(\sum_{\tau=0}^{T-1} \left(\sum_{j=1}^{T-\tau} \boldsymbol{b}(j) \boldsymbol{b}(j+\tau) \right) (\boldsymbol{\Sigma}_{\boldsymbol{1}}^{\boldsymbol{\tau}} + \boldsymbol{\Sigma}_{\boldsymbol{2}}^{\boldsymbol{\tau}}) \right) \boldsymbol{\omega} = 1 \tag{27}$$

Since $\boldsymbol{b}(1)=1$, a T-1 dimensional problem remains which can be solved using optimization techniques like gradient or line-search methods if T is not too large. Consequently we get for each class a frequency band filter and a spatial pattern.

In order to avoid overfitting it is necessary to enforce a sparse solution for b. Sparsity of is achieved by introducing a regularization term in the following way:

$$\max_{b} \max_{\omega} \boldsymbol{\omega}^{\mathrm{T}} \left(\sum_{\tau=0}^{T-1} \left(\sum_{j=1}^{T-\tau} \boldsymbol{b}(j) \boldsymbol{b}(j+\tau) \right) \boldsymbol{\Sigma}_{\boldsymbol{1}}^{\boldsymbol{\tau}} \right) \boldsymbol{\omega} - C/T \|\boldsymbol{b}\|_1 \tag{28}$$

under the same condition as (26). Here C is a non-negative regularization constant, which has to be chosen, e.g. by cross-validation. With higher C we get sparser solutions for $\boldsymbol{b}$ until at one point the usual CSP approach remains.

4.3. Matlab software for CSP and CSSSP comparative analysis

In this thesis we investigated the advantages of CSP and its counterpart CSSSP on three different high density datasets. For this purpose we have developed the Matlab software with graphical user interface. The idea behind the software was to have the results from both algorithms on the same dataset in one interface. This way their differences and similarities are more apparent than by executing separate programs and saving the results with each execution of the script so they could be analyzed at later time. The graphical interface of the developed Matlab software is shown on Fig 4.2.

Prior to starting the program, we had to import the data written in an OV file into Matlab. Since this data format is unreadable to Matlab Engine we converted it to GDF file which can be read by means of the *EEGlab* toolbox in Matlab. Conversion of OV to GDF file is done in an OpenViBE script using the already existing boxes from this program.

Once the GDF data is loaded into *EEGlab* the preprocessing of the data can be done in this toolbox. By choosing the filtering option and specifying the FIR parameters we bandpass filtered the data in 7-30 Hz frequency range. The sampling rate can also be changed at this point, however, in this thesis we retained the sampling rate of 500Hz which is the hardware sampling frequency. After the successful filtering, the data was separated into two matrices, one designated for left and the other for right hand trials, according to the markers inserted by *Graz Motor Imagery BCI Stimulator* box in OpenViBE. These two matrices were then saved as Matlab structure files (*.mat) which can be accessed by other Matlab scripts. Data from the structure file is a matrix $\boldsymbol{S_l} \in \mathbb{R}^{chxtxn_l}$, where *ch* is a number of recorded channels, *t* is a number of samples in one trial and n_l is a total number of trials in one out of two classes.

At this point the program we created can be started. The opening screen is divided into four panels. The first, upper left panel, called *'Convert EEGlab data'* is used to create training and testing sets when the matrices with left and right hand trials are loaded. When the first two buttons in this panel are pressed (*'Choose left hand data'* and *'Choose right hand data'*), a search window opens and the user chooses the needed matrices. Based on these two matrices which originated from the same subject in the same session, training and testing sets are obtained by pressing the button *Convert*. Data is divided into testing and training sets in equal distribution, meaning that there is the same number of left hand and right hand trials in one of the sets. Furthermore, the training set we created in this way contains four times more data then the testing set.

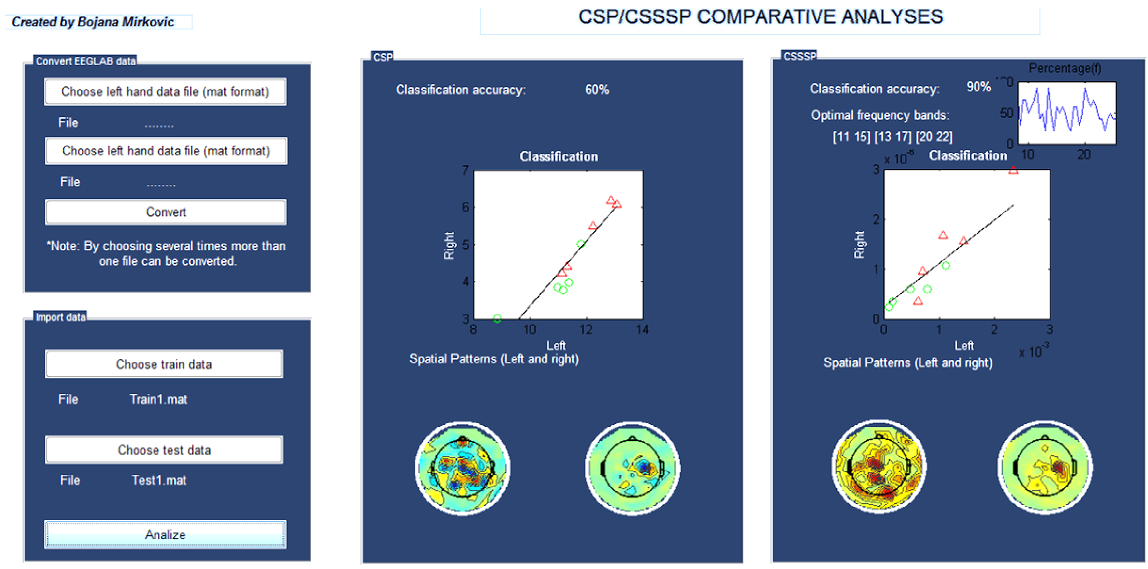

Figure 4.2. Graphical user interface for comparative analysis of CSP and CSSSP method

Both sets are saved in the Matlab structure format so this panel can be avoided if the same file needs to be processed again in the future.

In case testing and training set already exist, the bottom left panel can be used to load them into program by pressing *'Choose train data'* and *'Choose test data'*. This step is not necessary if the data is first converted using the *'Convert EEGlab data'* panel, and those datasets will be used instead. However, even if the data was previously converted, button *'Analyze'* must be pressed in order to perform CSP and CSSSP algorithms.

We performed the CSP analysis in accordance with equations (3)-(14) which present a basic Common Spatial Pattern algorithm, while the CSSSP is done using the methods explained through equations (24-27). The signals with delayed trials are produced using the *proc_AddDelayedChannels.m* function integrated into the *BBCI* Matlab toolbox. The delay for each of the 15 delayed channels is set to 2 ms. We found the corresponding 16 element frequency filter $\boldsymbol{b}$ as the FIR bandpass filter in 8-10 Hz range. After that we calculated the covariance matrix by (24) and (25), finally applying the usual CSP algorithm on the resulting data (27). We performed the classification on the testing data and saved the accuracy percentage in a designated array. In the next step, we increase the FIR frequency band by 1 Hz and then by 2 Hz, and after each change the same procedure is repeated with different filters. After this the low edge of the FIR filter is increased by 1 Hz up to 25 Hz, while for each new low edge the width of the filter varies from 2 to 4 Hz. The band which results in the best classification is most likely the alpha band of the given subject, and the corresponding decomposition matrix is used as the result of CSSSP algorithm.

Once we had obtained the decomposition matrix from the analysis on the training set, we extracted the feature vectors using the first and last column of the decomposition matrix each maximizing/minimizing the difference of trial variance (29). Feature vectors are also extracted from the testing set using the same decomposition matrix $\boldsymbol{\omega}$. For the CSSSP for each frequency a different decomposition matrix is obtained.

$$\boldsymbol{f}_{\boldsymbol{v}_{\boldsymbol{y}}} := \left(\langle \log(1 + \frac{\sum_{i=1}^{t} \boldsymbol{\omega}_k^T \boldsymbol{S}_{\boldsymbol{y},\boldsymbol{i}}}{t}) \rangle \, | k \in \{1, \dim(\boldsymbol{\omega})\} \right) \tag{29}$$

For classification of feature vectors we used the linear discriminant analysis. The predefined Matlab function *classify.m* calculates the coefficients of the linear classifier according to the input feature vectors of testing and training data. The visual representation of classification can be seen in the middle plot of the third panel for CSP algorithm and in the middle plot of the fourth panel for CSSS. In the second plot the data is plotted with regard to the frequency band which results in the best classification. The right hand trials are marked with red triangles on these plots, while left hand trials are marked with green circles.

The percentage of accurately sorted trials from the testing set can be seen in the top of the third panel for the CSP algorithm and the top of the fourth panel for the CSSSP algorithm. In case of the CSSSP algorithm, the highest percentage indicates which bandpass filter should be applied. The plot next to the classification accuracy shows the accuracy percentage for all frequency ranges, or tested filters.

At the bottom of both algorithm panels the topoplots of Common Spatial Patterns are presented.

5. RESULTS OF THE COMPARATIVE ANALYSIS

The successfulness of the CSSSP algorithm when comparing it to the original CSP algorithm will be demonstrated in the following chapter. The table view of advantages and disadvantage will be given, in addition to graphical presentation of trial data classification.

Originally we used four datasets for the analysis. One was obtained during the training session of one subject while the other three were all recorded from another subject (two of which during the feedback session and one during the training session). We visually tested all of the datasets for any remaining artefacts after the wide range filtering (7-30Hz). In case any artefacts remained after the filtering they were removed as a part of the preprocessing. Due to the very low accurate classification rate using both the CSP and CSSSP analysis, one dataset was removed from the whole experiment.

The first and somehow most important criterion for measuring the performance of any algorithm would be its success rate, or in the case of motor imagery study classification accuracy. In Table 5.1 the classification results are given, obtained from the three 10-trial testing sets and three 30-trial training sets as well as using the 12-trial testing set and 28-trial training set. It should be mentioned that the choice of training and testing set and its mutual ratio has a fair impact on the analysis itself. In case of the bigger testing set, more classification mistakes will be present.

Table 5.1. Classification accuracy using the CSP and CSSSP method

	training/testing ratio=3		training/testing ratio=2.33	
	CSP [%]	CSSSP [%]	CSP [%]	CSSSP [%]
Dataset 1	60	90	50	67
Dataset 2	60	80	58,34	58,34
Dataset 3	70	80	66,67	91,67

It can be clearly seen that the CSSSP method is in most cases by far superior to the CSP. This result somewhat differs in performance to [24] where the difference between both algorithms varies from 1 to 15%. This difference may be the cause of a modified motor imagery paradigm, the trial distribution in testing and training data, the data quality, or simply the amount of data available for training session.

However, the accurate classification percentage is sometimes insufficient for further analyses. Therefore, in our software we have shown the graphical presentation of testing data feature vectors divided by a classifier line. By plotting two hyperplanes the hyperplane distance can be observed for each trial and with it the certainty of classification. Of course, this result also depends on the subject's success in performing the task during the trial, so the hyperplane distance may be great but at the same time the trial classified in the wrong class. CSSSP shows better results in this area too, since it relies only on data filtered in the narrow frequency band which results in the best classification and is more likely the result of motor imagery itself. Therefore, during the analysis of the feature vector plots the accurate classification should also be taken into account. The graphical feature vector presentation of three datasets, using the 10-trial testing data can be seen on Fig 5.1-Fig 5.12.

From the first two datasets we have shown that CSSSP has indeed done better classification than CSP. While the hyperplane distance may in some cases be greater in the case of CSP one can notice that those individual trials can be the result of wrong classification, which is not the case with CSSSP. The third dataset does show better results if the hyperplane distance is observed, however, the overall classification is certainly better with CSSSP.

CSP

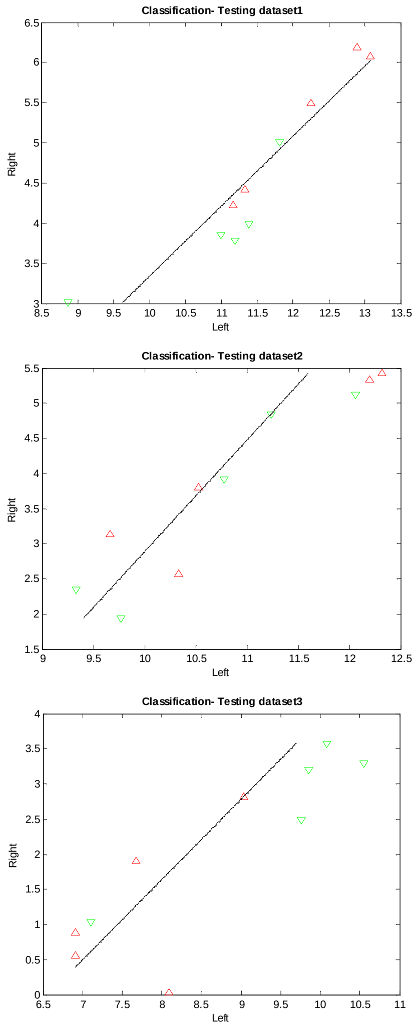

Figures 5.1.-5.6. Testing set feature vector distribution separated by a linear classifier. Feature vectors were obtained using the basic CSP analysis.

CSSSP

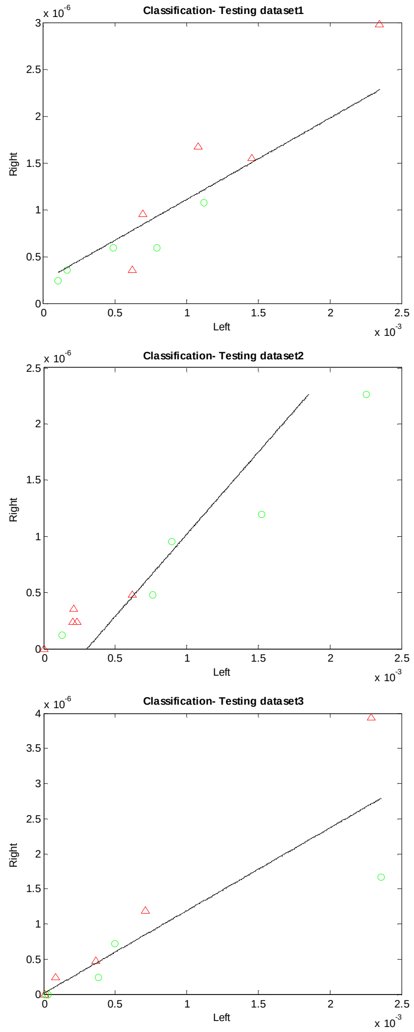

Figures 5.7.-5.12. Testing set feature vector distribution separated by a linear classifier. Feature vectors were obtained using the CSSSP analysis.

It is expected that most of the motor imagery activity can be detected over the sensorymotor cortex, located at the border of parietal lobe. According to previous studies and motor homunculus, the optimal electrode positions for motor imagery are C3 and C4. Nevertheless, this may vary from subject to subject, and sometimes can even change between two separate sessions. The Common spatial patterns can indicate the cortex regions which maximize and minimize the trial variance for both left and right trials, providing the valuable information about activated regions. The distribution acquired from the previous three datasets with high density 96 channel data can be seen on Fig 5.13-5.24.

Another disadvantage of the basic CSP method lies in its inability to detect the frequency range of interest. The results are based on the data filtered in 7-30 Hz frequency band during the preprocessing. On the other hand, in CSSSP a decomposition matrix with the highest classification accuracy returns the frequencywise valuable result. This way, CSSSP detects the frequencies where the alpha or beta activity appears, since both may be connected with motor tasks. The algorithm returns more than one frequency band in case their analysis produce the same, highest, classification accuracy. As it is, most of the best suited filters suggested by CSSSP are indeed in these two bands, confirming this algorithm's superiority over its counterpart's. The specific results for the separate datasets are shown in Table 5.2.

Table 5.2. Frequency bands which produce the highest classification accuracy, as suggested by the CSSSP algorithm

	Filter in alpha range	Filter in beta range
Dataset 1	11-15	20-22
Dataset 2	12-14	21-23
Dataset 3	12-14	-

CSP

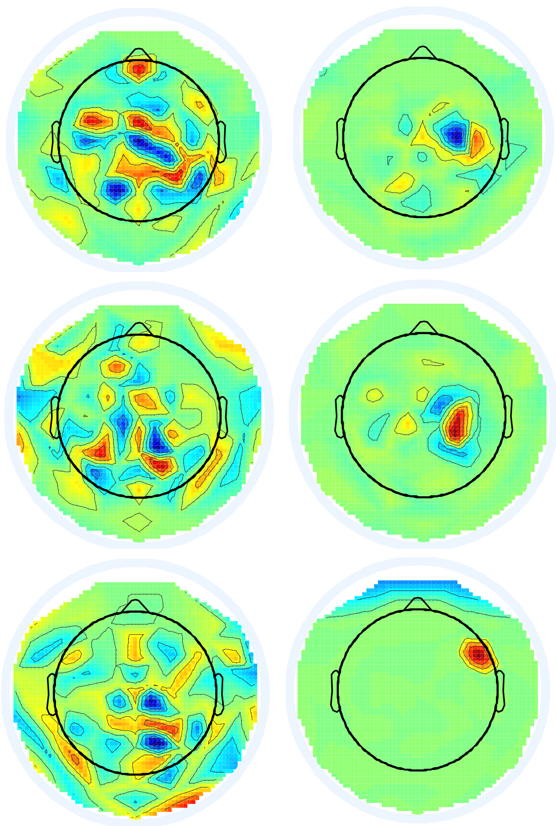

Figures 5.13.-5.18. Common Spatial Patterns obtained by the basic CSP algorithm (the spatial activity distribution for left hand imagery is shown in the left column and for right hand imagery in the right column)

CSSSP

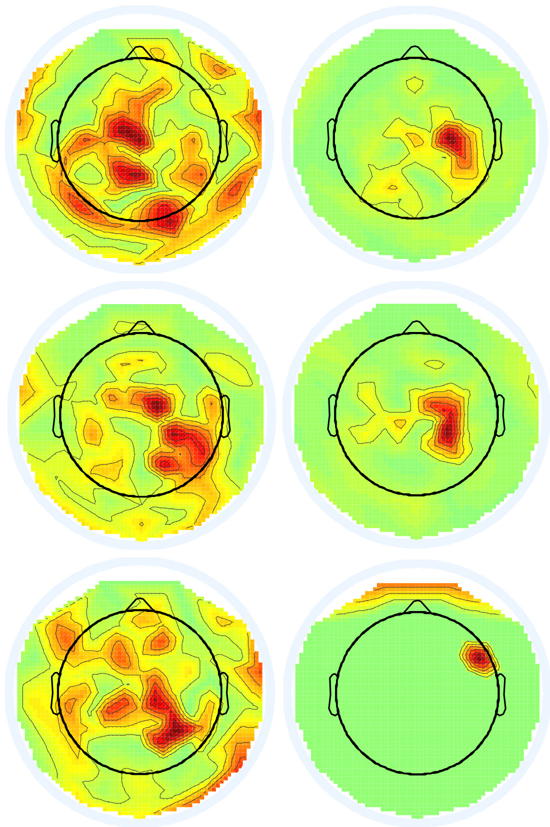

Figures 5.19.-5.24. Common Spatial Patterns obtained by the CSSSP algorithm (the spatial activity distribution for left hand imagery is shown in the left column and for right hand imagery in the right column)

A very noticeable advantage of the basic CSP algorithm definitely lies in its speed. The whole classification process with basic CSP takes only 0.2 seconds to execute on the average personal computer. As opposed to that the CSSSP for the frequency band detection and classification takes 20.3 seconds for processing the dataset of the same size. For many application purposes this may even be the crucial factor when choosing between these two algorithms, so the basic CSP should not be underestimated in any way.

6. CONCLUSION

The focus of this master thesis is on achieving the most successful classification during the motor imagery experiment. This task does not only include the processing of recorded EEG signals, but also the most efficient motor imagery paradigm, visual feedback and a choice of an adequate processing tool.

The first unavoidable task which must be overcome, the provision of realistic feedback, was solved in this thesis by using the hand movement of LEGO Mindstorms NXT robot. We did the robot configuration and programming in the way that would be most suited for such EEG session, taking all the possible downsides in consideration and successfully turning them into advantages.

Second part of the thesis deals with the most important question in all BCI techniques, the most beneficial algorithms for EEG signal processing with regard to commendable ensuing classification. Nowadays, two of the most frequently applied algorithms include Common Spatial Pattern and Common Sparse Spatio Spectral Pattern. The question, however, remains which of the two should be used in which circumstances and how efficient these algorithms really are in discriminating two classes from preprocessed EEG recordings.

Our extensive analysis of both algorithms has shown a definite superiority of CSSSP algorithm over its counterpart, due to its encompassing adaptive spectral filtering and possibility to detect alpha and in some cases beta activity bands in every subject. However, even if this algorithm shows exceptional results it is not best suited if time is of the essence, or only rudimentary analysis is required. In these cases it is beneficial to resolve the matter of classification by means of the CSP which is by far faster, whereas only some accuracy will be forgone in return.

Applying the proposed signal processing techniques increases the accuracy of motor imagery classification performed in this thesis up to 91.7% with the CSSSP, which is better than most known spatial and temporal filters for multivariate time-series can accomplish.

Until novel spatio-temporal filtering methods are developed, we have shown that the CSSSP remains one of the leading methods for interpreting the noisy data with overlapping frequency ranges by utilizing optimal combination of spatial and spectral filters.

7. LITERATURE

[1] D. Popović, M. Popović, M. Janković, "Biomedicinska merenja i instrumentacija", *Akademska misao*, Belgrade, ISBN 978-86-7466-371-4, 2010

[2] M. DeVos, S. Riès, K. Vanderperren, B. Vanrumste, F.X. Alario, S. Van Huffel , B. Burle, "Removal of muscle artifacts from EEG recordings of spoken language production", *Neuroinformatics*, 8:135-150., DOI 10.1007/s12021-010-9071-0, 2010

[3] D.L. Schomer, F.L. Da Silva, "Niedermeyer's electroencephalography: basic principles, clinical applications, and related fields", *Lippincott Williams & Wilkins*, 6th Edition, ISBN 978-0781789424, 2010

[4] B. Mirković, "Detekcija zamišljenih pokreta ruku i nogu iz kortikalnih signala", Bachelor thesis, Belgrade, 2012

[5] G. Pfurtscheller, C. Neuper, "Motor imagery and direct brain-computer communication", *Proceedings of the IEEE*, 89(7), 1123-1134., DOI 10.1109/5.939829, 2001

[6] S. de Vries, T. Mulder, "Motor imagery and stroke rehabilitation: a critical discussion", *Journal of Rehabilitation Medicine*, 39(1), 5-13., PMID 17225031, 2007

[7] R. W. Williams, K. Herrup, "The control of neuron number", *Annual Review of Neuroscience* 11: 423–53. DOI 10.1146/annurev.ne.11.030188.002231. PMID 3284447, 1988

[8] R. Toro, M. Perron, B. Pike, L. Richer, S. Veillette, Z. Pausova, T. Paus, "Brain size and folding of the human cerebral cortex", *Oxford Journals, Life Sciences & Medicine, Cerebral Cortex*, Volume 18, Issue 10, Pp. 2352-2357, DOI 10.1093/cercor/bhm261, 2008

[9] O. Simon, J.F. Mangin, L. Cohen, D.L. Bihan, S. Dehaene, "Topographical layout of hand, eye, calculation, and language-related areas in the human parietal lobe", *Neuron* 33.3 : 475., PMID 11832233, 2002

[10] J. Duncan, A.M. Owen, "Common regions of the human frontal lobe recruited by diverse cognitive demands", *Trends in neurosciences*, PMID 11006464, 2000

[11] "Guideline seven: a proposal for standard montages to be used in clinical EEG. American Electroencephalographic Society", *Journal of Clinical Neurophysiology* 11(1):30–6. DOI 10.1097/00004691-199401000-00008. PMID 8195424, 1994

[12] J.R. Wolpaw, N. Birbaumer, W.J. Heetderks, D.J. McFarland, P.H. Peckham, G. Schalk, T.M. Vaughan, "Brain-computer interface technology: a review of the first international meeting", *IEEE transactions on rehabilitation engineering*, 8(2), 164-173., DOI 10.1109/TRE.2000.847807, 2000

[13] http://upmc.com/media/media-kit/bci/Pages/default.aspx, 2013

[14] G. Buzsáki, "Theta oscillations in the hippocampus", *Neuron* 33(3):325–40, DOI 10.1016/S0896-6273(02)00586-X. PMID 11832222., 2002

[15] Heung-Il Suk, Seong-Whan Lee, "A Novel Bayesian Framework for Discriminative Feature Extraction in Brain-Computer Interfaces", vol.35 no.2 pp.286-299 DOI 10.1109/TPAMI.2012.69, 2013

[16] C. Neuper, R. Scherer, S. Wriessnegger, G. Pfurtscheller, "Motor imagery and action observation: modulation of sensorimotor brain rhythms during mental control of a brain–computer interface", *Clinical neurophysiology*, 120(2), 239., DOI 10.1016/j.clinph.2008.11.015, 2009

[17] F. Lotte, G.Cuntai ,"Regularizing common spatial patterns to improve BCI designs: unified theory and new algorithms." *Biomedical Engineering, IEEE Transactions on* 58.2 (2011): 355-362., 2010

[18] "LEGO Mindstorms NXT 2.0 User guide and specification", http://mindstorms.lego.com/en-us/products/default.aspx, 2013

[19] "OpenViBE designer documentation", http://openvibe.inria.fr/tutorial-the-most-basic-openvibe-setup, 2013

[20] K. Fukunaga, Keinosuke, "Introduction to statistical pattern recognition", *Academic press*, ISBN 9780080478654, 1990.

[21] H. Ramoser, J. Muller-Gerking, G. Pfurtscheller, "Optimal spatial filtering of single trial EEG during imagined hand movement", Rehabilitation Engineering, IEEE Transactions, 8(4), 441-446., DOI 10.1109/86.895946, 2000

[22] S. Lemm, B. Blankertz, G. Curio, K.R. Muller, "Spatio-spectral filters for improving the classification of single trial EEG", Biomedical Engineering, IEEE Transactions, 52(9), 1541-1548., DOI 10.1109/TBME.2005.851521, 2005

[23] G. Dornhege, B. Blankertz, M. Krauledat, F. Losch, G. Curio, K.R. Muller, "Combined optimization of spatial and temporal filters for improving brain-computer interfacing", Biomedical Engineering, IEEE

Transactions, 53(11), 2274-2281., DOI 10.1109/TBME.2006.883649, 2006

[24] B. Blankertz, R. Tomioka, S. Lemm, M. Kawanabe, K.R. Muller, "Optimizing spatial filters for robust EEG single-trial analysis"., Signal Processing Magazine, IEEE, 25(1), 41-56., DOI 10.1109/MSP.2008.4408441 2008

[25] B. Reuderink, M. Poel, "Robustness of the common spatial patterns algorithm in the BCI-pipeline".,2008

[26] G. Pfurtscheller, R. Scherer, R. Leeb, C. Keinrath, C. Neuper, F. Lee, "Viewing moving objects in virtual reality can change the dynamics of sensorimotor EEG rhythms", Presence Teleop Virt Environ 16(1):111–8., DOI 10.1162/pres.16.1.111, 2007